Neuron
NeuroResource

A Quantitative Framework to Evaluate Modeling of Cortical Development by Neural Stem Cells

Jason L. Stein,[1,7] Luis de la Torre-Ubieta,[1,7] Yuan Tian,[1] Neelroop N. Parikshak,[1] Israel A. Hernández,[2] Maria C. Marchetto,[3] Dylan K. Baker,[1] Daning Lu,[1] Cassidy R. Hinman,[4] Jennifer K. Lowe,[1] Eric M. Wexler,[1] Alysson R. Muotri,[5] Fred H. Gage,[3] Kenneth S. Kosik,[6] and Daniel H. Geschwind[1,*]

[1]Neurogenetics Program, Department of Neurology, Center for Autism Research and Treatment, Semel Institute, David Geffen School of Medicine, University of California, Los Angeles, Los Angeles, CA 90095, USA
[2]Neuroscience Research Institute, University of California, Santa Barbara, Santa Barbara, CA 93106, USA
[3]Laboratory of Genetics, Salk Institute for Biological Studies, La Jolla, CA 92037, USA
[4]Center for Stem Cell Biology and Engineering, University of California, Santa Barbara, Santa Barbara, CA 93106, USA
[5]School of Medicine, Department of Pediatrics/Rady Children's Hospital San Diego, Department of Cellular & Molecular Medicine, Stem Cell Program, University of California, San Diego, La Jolla, CA 92093, USA
[6]Molecular, Cellular and Developmental Biology and Neuroscience Research Institute, University of California, Santa Barbara, Santa Barbara, CA 93106, USA
[7]Co-first Authors
*Correspondence: dhg@mednet.ucla.edu
http://dx.doi.org/10.1016/j.neuron.2014.05.035

SUMMARY

Neural stem cells have been adopted to model a wide range of neuropsychiatric conditions in vitro. However, how well such models correspond to in vivo brain has not been evaluated in an unbiased, comprehensive manner. We used transcriptomic analyses to compare in vitro systems to developing human fetal brain and observed strong conservation of in vivo gene expression and network architecture in differentiating primary human neural progenitor cells (phNPCs). Conserved modules are enriched in genes associated with ASD, supporting the utility of phNPCs for studying neuropsychiatric disease. We also developed and validated a machine learning approach called CoNTExT that identifies the developmental maturity and regional identity of in vitro models. We observed strong differences between in vitro models, including hiPSC-derived neural progenitors from multiple laboratories. This work provides a systems biology framework for evaluating in vitro systems and supports their value in studying the molecular mechanisms of human neurodevelopmental disease.

INTRODUCTION

Human neural stem cells are poised to revolutionize our ability to make mechanistic inferences, bridging the gap between traditional model systems and human biology (Dolmetsch and Geschwind, 2011; Merkle and Eggan, 2013). Ideally, such a platform should maximize translational potential by recapitulating in vivo brain development and function as much as possible. Human embryonic stem (hES), induced pluripotent stem (hiPS), and primary human neural progenitor (phNPC) cells all have the ability to differentiate into functional neurons (Espuny-Camacho et al., 2013; Hansen et al., 2011; Palmer et al., 2001; Sandoe and Eggan, 2013). In each of these systems, disease-related processes can be modeled and studied by either generating hiPSCs from patients with known mutations or introducing genetic modifications into control neural stem cell lines (An et al., 2012; Brennand et al., 2011; Israel et al., 2012; Marchetto et al., 2010; Paşca et al., 2011; Rosen et al., 2011; Ryan et al., 2013; Soldner et al., 2011). Despite many options, there is neither a clear consensus as to which system or culture conditions are better suited to model aspects of neurodevelopment and disease nor a rubric for answering this question. The following have not been demonstrated using a rigorous genome-wide statistical framework: (1) how well in vitro models match in vivo development, (2) what level of developmental maturity is achieved after differentiation, (3) what neuroanatomical identity is modeled, (4) what specific neurodevelopmental processes and molecular mechanisms are preserved, and (5) what specific aspects remain to be better modeled in vitro, providing a guide for future work optimizing in vitro systems.

Recent large-scale efforts to measure the transcriptome from postmortem human brain provide an unbiased in vivo standard to which in vitro systems can be compared. These data sets measure gene expression at time points from embryonic to late adulthood and across several cortical and subcortical regions (Kang et al., 2011). In addition, gene expression in microdissected cortical laminae has been measured at mid to late fetal time periods (Miller et al., 2014), providing data sets with increased spatial resolution within a restricted developmental window.

Here, we develop and demonstrate genome-wide methods to quantify the similarity between in vitro neural stem cell models and brain development in vivo and apply them to a newly generated set of phNPC lines. We demonstrate remarkable preservation of neurodevelopmental processes spanning embryonic to fetal corticogenesis in phNPCs in vitro. But, even after months

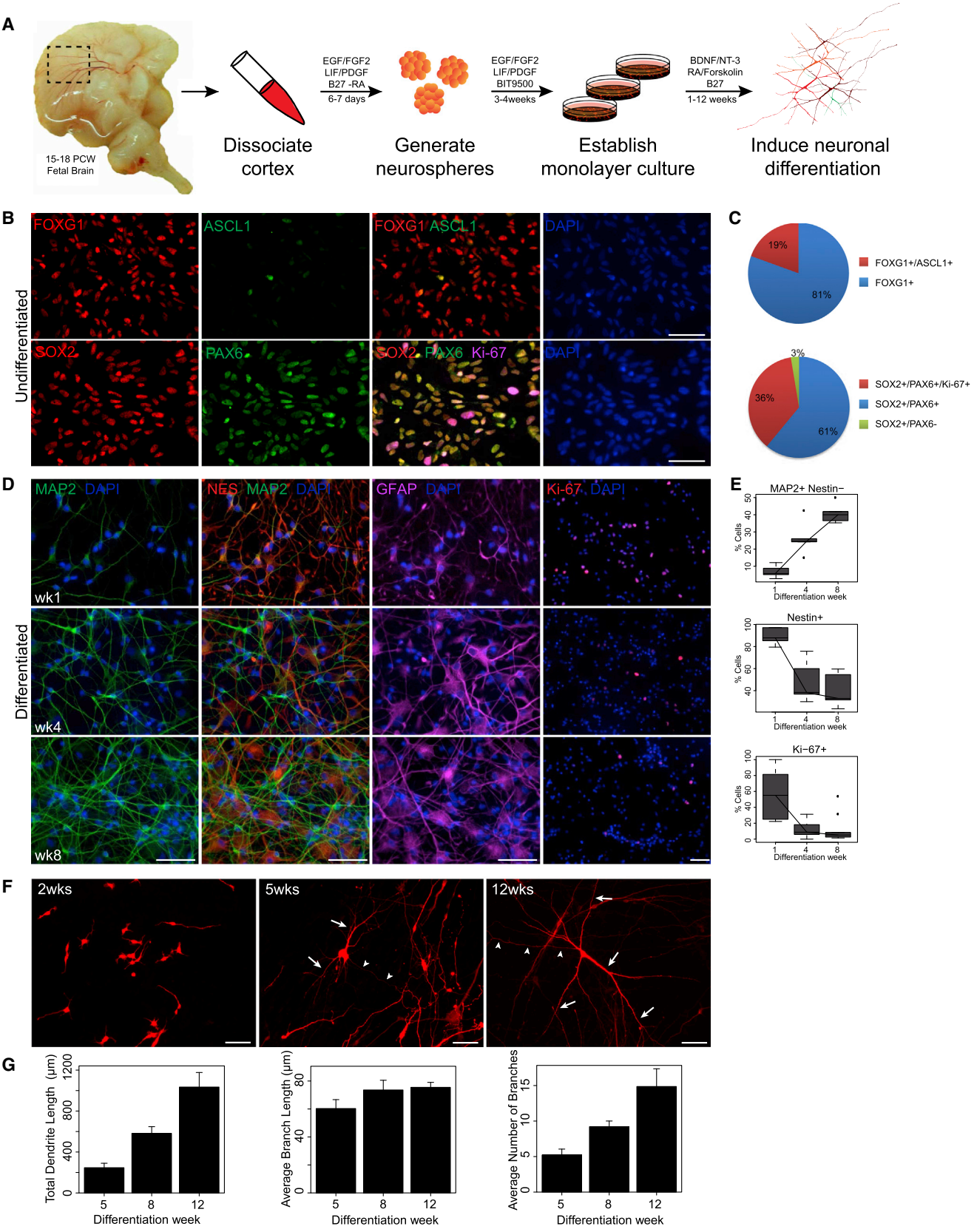

(legend on next page)

in a dish, neither phNPCs nor hiPSC-derived neurons mature beyond fetal stages. We further uncover gene expression networks driving these processes, show their preservation in vitro, and reveal they are enriched in autism spectrum disorders (ASDs) risk genes. Finally, we expand this analysis to hiPSC- and hES-based neural stem cell models and find striking differences in overlap to in vivo development and preservation of network architecture. We have implemented this framework into a user-friendly website (http://context.semel.ucla.edu/) as a resource for the community.

RESULTS

phNPCs Express Telencephalic Markers and Undergo Stereotypical Neuronal Morphogenesis upon Differentiation

We generated phNPC lines from 15–18 postconception week (PCW) human fetal brains by a neurosphere isolation method (Konopka et al., 2012; Palmer et al., 2001; Rosen et al., 2011; Wexler et al., 2011) (Figure 1A; Experimental Procedures available online). All lines were genotyped to determine sex and to exclude samples with aneuploidy. Immunostaining of undifferentiated phNPCs was consistent with standard methods used to define dorsal telencephalic progenitors/radial glia of human cortex (Hansen et al., 2010) (Figures 1B and 1C). During differentiation, the typical progression of decrease in mitotic and neural stem cell markers (Ki-67 and NES) with concomitant increase in neuronal markers (Tuj1, DCX, and MAP2) during cortical maturation was observed (Figures 1D and 1E; data not shown). We also detected cells expressing TBR2, a marker of intermediate progenitor cells (Englund et al., 2005; Hansen et al., 2010), all of which costained with PAX6, consistent with the immunocytochemical profile of the ISVZ (Betizeau et al., 2013; Fietz et al., 2010) (data not shown). The in vitro expression profile of genes marking laminar potential and fate across differentiation was also consistent with sequential generation of lower and upper layer projection neurons during corticogenesis (Arlotta et al., 2005; McEvilly et al., 2002) (Figures S1A–S1C). In addition, phNPCs generate neurons with stereotypical morphologies similar to what is observed in vivo, first forming bipolar migrating cells, followed by axonogenesis and increases in dendritic arborization (Figures 1F and 1G).

Few commonly used literature-based markers are specific to a single region (Figure S2A). For instance, PAX6 is widely used as a dorsal telencephalic marker (Espuny-Camacho et al., 2013; Paşca et al., 2011), as it largely separates the dorsal pallium from ventral pallium, but it is also strongly expressed in other brain regions, including the developing diencephalon and hindbrain (Manuel and Price, 2005) (Figure S2A). To overcome this limitation, we generated a list of genes enriched in different brain regions based on transcriptomic data from human brain (Kang et al., 2011) (Supplemental Experimental Procedures) and used these gene sets as an initial standard. Cortical regional markers were highly expressed in all phNPC lines, while expression of markers of other brain regions was much lower (Figure 2). Further, expression of the majority of literature-based markers was also very similar between in vivo cortex and phNPCs (Figures S2B and S2C), further validating the cortical identity of phNPC cultures using an unbiased approach.

Mapping In Vitro Differentiation of phNPCs to In Vivo Cortical Development

We next developed an unbiased genome-wide transition mapping (TMAP) approach to assess the extent of overlap between in vivo cortical development and in vitro differentiation. TMAP consists of serialized differential expression analysis between any two in vivo developmental periods defined from a spatiotemporal transcriptomic atlas (Kang et al., 2011) and any two in vitro differentiation time points, followed by quantification of overlap using the rank-rank hypergeometric overlap test (Plaisier et al., 2010) for each combination of time periods. This method has the advantage of allowing for a threshold-free (1) identification of which in vivo developmental transition best overlaps with differentiating phNPCs and (2) statistical assessment of the extent of overlap. This technique generates a map of the overlap between any two systems across development.

We applied TMAP, comparing a signed, p value-ranked list of differentially expressed (DE) genes over 12 weeks of differentiation in vitro to genes DE between the listed developmental periods from human cortex (Figure 3A) and observed strong overlap between phNPC and cortical developmental periods up to late mid-fetal periods (max $-\log_{10}$(p value) > 460). The strong matching observed in transitions from period 1 or 2 is consistent with the differentiation of the progenitor-enriched week 1 postdifferentiation (PD) time point (Figure 1C), since the in vivo data set only includes cortical germinal zones in periods 1 and 2 (Kang et al., 2011). Genes coordinately upregulated in vitro and in vivo driving the overlap are related to processes of normal neuronal differentiation, whereas codownregulated genes are related to mitosis, cell-cycle arrest, and carbohydrate utilization (Figures 3B and 3C).

Examples of key candidate genes that have preserved rankings show remarkably similar trajectories of gene expression

Figure 1. phNPCs Express Canonical Telencephalic Markers and Undergo Stereotypical Neuronal Morphogenesis

(A) Isolation, culture, and differentiation of phNPCs from human fetal cortex.

(B and C) Isolated phNPCs express dorsal telencephalic and radial glia markers. Undifferentiated phNPCs were subjected to immunocytochemistry with the indicated antibodies and the DNA-binding dye 4′,6-diamidino-2-phenylindole (DAPI). Telencephalic (FOXG1, 100%, ASCL1, 19%; n = 368 cells), dorsal telencephalic and radial glia (PAX6, SOX2; 97%, n = 395 cells), and mitotic (Ki-67; 36%, n = 395 cells) markers are expressed.

(D and E) Differentiation of phNPCs into MAP2+ neurons with concomitant decrease in neural progenitors (Nestin, Ki-67) across the indicated time points (n = 794 cells; Ki-67, n = 1,693 cells). Box plot whiskers encompass all points within 1.5 × (interquartile range).

(F) phNPCs were infected with a low titer of turboRFP-expressing lentivirus (pTRIPZ) and subjected to immunocytochemistry with MAP2 and turboRFP antibodies at 2, 5, and 12 weeks postdifferentiation. Axo-dendritic polarization and increased dendritic complexity is observed over development in vitro. Arrows and arrowheads indicate dendrites and axons, respectively.

(G) Quantification of dendrite morphogenesis in MAP2+ neurons treated as in (F) shows robust dendrite growth and branching over differentiation (n = 23 cells/time point in five lines from three donors; mean ±SEM displayed in barplot). Scale bar equal 50 μm for all panels.

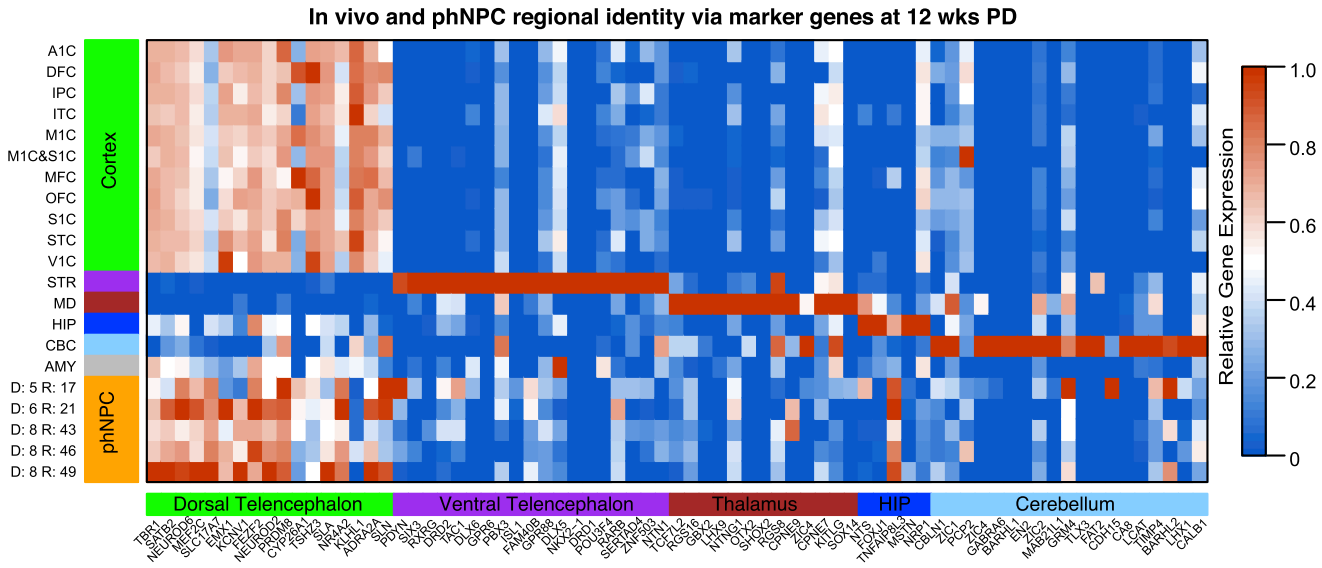

Figure 2. Expression of Transcriptomically Defined Regional Markers In Vitro and In Vivo

Expression levels of 5 to 20 marker genes enriched in each indicated brain region during late mid-fetal in vivo development (Period 6) along with 12 week PD phNPCs are shown. Genes are shown on the x axis with colors to indicate the region for which the gene is a marker. The y axis indicates the in vivo dissected region or in vitro cell line, specified by donor identification number and region identification number. Relative expression is indicated by color within the heat map and normalized for each gene from 0 to 1. Cortex: OFC, DFC, VFC, MFC, M1C, S1C, IPC, A1C, STC, ITC, and V1C; Hippocampus: HIP; Amygdala; AMY; Striatum: STR; Medial Dorsal Nucleus of the Thalamus: MD; and Cerebellar Cortex: CBC.

when compared to in vivo development up to period 6 (Figure 3C). Mapping the in vitro transitions between periods 1 to 4, periods 4 to 8, and periods 8 to 12 weeks PD to in vivo developmental periods allows for visualization of the progressive maturation of phNPCs cultures (Figure S3B). It is evident that later transitions in differentiation correspond to later periods of human development.

Next, we sought to apply this same TMAP tool to transcriptomes derived from laser capture microdissection of cortical laminae from postmortem human fetal brain (15–21 PCW) (Miller et al., 2014), permitting a direct assessment of in vivo matching between cortical neural progenitors and their postmitotic derivatives. The transition between 1 and 12 weeks PD in differentiating phNPCs has strongest correspondence to the transition between the ventricular zone or subventricular zone to subplate and inner cortical plate (Figure 3D). As expected, this overlap is largely driven by synaptic genes coordinately upregulated and cell-cycle genes codownregulated during the transition between subventricular zone and inner cortical plate in vivo and the transition between 1 and 12 week PD in vitro (Figure 3E).

Individual In Vitro Sample Prediction of Regional Identity and Developmental Period

The above analyses perform group-based determination of developmental period. We sought to develop an approach that would allow determination of these features in individual samples, thus precluding the need to pool samples into groups or to compare between specific stages or transitions. We developed a multilabel (developmental period and regional identity), multiclass (periods: 1–15; regions: cortex, hippocampus, amygdala, thalamus, striatum, and cerebellum) machine learning framework (Tsoumakas and Katakis, 2007), named *C*lassification *o*f *N*euroanatomical and *T*emporal *Ex*pression via *T*ranscriptomics (CoNTExT), for this purpose. We trained the algorithm on a spatiotemporal transcriptome atlas of the human brain (Kang et al., 2011) (Figure 4A). After feature selection and parameter optimization (Experimental Procedures), cross-validation accuracy in the training data set was high (10-fold cross-validation with 90% split percentage; exact accuracy for developmental period: 99.6%; accuracy for regional identification: 96.9%).

We then applied this recognition algorithm to four other data sets of transcriptional profiling from postmortem human brain to provide independent validation (Hernandez et al., 2012; Israel et al., 2012; Johnson et al., 2009; Liu et al., 2012), attaining high levels of accuracy in each of these new data sets, despite differences in microarray platforms, processing of samples, and laboratories (Figures 4A, 4B, and S4A–S4C). Importantly, in the same platform as the in vitro phNPCs data (Illumina HT-12 Beadchip), the algorithm was able to correctly classify both fetal (Figure S4B) (Israel et al., 2012) and adult brain (911 samples; Figure S4C) (Hernandez et al., 2012). Overall, CoNTExT is accurate at differentiating distinct in vivo developmental epochs from each other (e.g., between early, mid, and late fetal; fetal versus newborn; childhood versus adolescence; and childhood versus adulthood).

We next applied CoNTExT to phNPC cultures to predict the developmental period and regional identity of each phNPC sample (see Supplemental Experimental Procedures). A progressive maturation of the culture can be seen across multiple differentiation weeks (Figure 4C). Similar to results from TMAP, but now for each single sample individually, we predict that these

cultures match most closely to embryonic development at 1 week PD and early to late mid-fetal development at 12 weeks PD. As in TMAP, the strong prediction of embryonic development at 1 week PD is likely due to the in vivo data set containing proliferative laminae of the cortex for these time periods only and the culture containing predominantly proliferative cells. In addition, regional prediction is strongly cortical, consistent with high expression of cortical markers in the developing phNPCs (Figure 1 and Figure 2).

Network Analysis Identifies Key Preserved Neurodevelopmental Processes in Differentiating phNPCs

Although TMAP and CoNTExT provide a cohesive framework to determine neuroanatomical region and developmental maturity, these methods are not tailored to characterize the preservation of specific cellular or biochemical processes. To identify which specific neurodevelopmental processes were preserved in vitro, we employed weighted gene coexpression network analysis (WGCNA). WGCNA identifies modules of coexpressed genes that correspond to shared function—for example, organelles, cell types, or biological processes. (Hawrylycz et al., 2012; Johnson et al., 2009; Kang et al., 2011; Miller et al., 2014; Oldham et al., 2008; Parikshak et al., 2013; Voineagu et al., 2011).

We constructed a network based on coexpression of genes in developing human cortex (Periods 1–8) (Kang et al., 2011) and assessed preservation of the network (Langfelder et al., 2011) (Experimental Procedures) in an independent in vivo data set of developing human cortex (Colantuoni et al., 2011) to identify the most robust and generalizable modules, identifying 28 well-preserved modules (Preservation Z score $\geq$4) (Table 1; Figure S5A). This network, defined in developing fetal cortex, represents a rubric for comparing in vitro development to in vivo development and identifying shared processes and mechanisms. We found that the majority of our high-confidence modules were strongly correlated with developmental period, but not as strongly with areal identity or hemisphere, suggesting modules are largely reflective of processes related to differentiation and maturation (Figure S5B).

We next assessed shared gene function within the module by enrichment of Gene Ontology (GO) terms, KEGG pathway analysis, and overrepresentation of genes in manually curated lists comprising key neurodevelopmental processes, brain cell populations, and their subcellular compartments (Figures 5B and S5D; Table 1). We identified modules related to major histogenetic and cellular processes driving cortical development, including exit from cell cycle (magenta, red, and grey60 modules), neurogenesis and differentiation (pink and magenta modules), axon growth and guidance and neuronal migration (purple, salmon, and green modules), dendrite growth (salmon and green modules), and synaptogenesis (green, salmon, lightgreen, cyan, paleturquoise, and yellow modules; Figures 5A and 5B; Table 1). The trajectory of gene expression over the developmental period (e.g., module eigengene), GO terms, and key hub genes are illustrated for a subset of these modules in Figure 5B. For instance, modules related to neural progenitor proliferation (magenta and pink) have eigengenes that decrease over time and contain mitotic checkpoint kinases as hubs (BUB1 and BUB1B; magenta) (Taylor and McKeon, 1997), as well as known markers of radial glia (PAX6, VIM, and NES; magenta); intermediate progenitors (EOMES; magenta); members of the Notch/delta signaling pathway NOTCH1 (magenta), NOTCH2, and HES1 (pink) (Kageyama et al., 2008); and members of the SHH signaling pathway (SMO, GLI2, and GLI3; magenta) (Sousa and Fishell, 2010). Interestingly, the pink module is also enriched in genes related to gliogenesis and astrocytes, including SOX8 and SOX9 (Kang et al., 2012; Stolt et al., 2003), and its eigengene is upregulated in late fetal development, consistent with the timing of gliogenesis in human cortex (Figures 5B and S5D) (Kriegstein and Alvarez-Buylla, 2009; Rakic, 2003).

A set of modules with trajectories of increasing expression over development mark different phases of neurogenesis. The purple module related to neuronal migration and axon guidance displays elevated expression during Periods 3–6, faithfully recapitulating the time period of these processes in vivo (Figure 5A), and contains the hub genes DCX and CRMP1, known to be involved in cytoskeleton regulation and neuronal migration (Gleeson et al., 1999; Goshima et al., 1995). Six additional modules are related to later phases of development, including axon and dendrite growth and synaptogenesis (purple, salmon, green, lightgreen, cyan, and paleturquoise). They contain hub genes involved in glutamatergic and GABAergic synapse function (Salmon: CAMK2β, GRIN1, GRID1, VAMP2, and SYT3/5; Green: GRIA4, GRIK4, GRIN3A, SHANK2, RIMS1, and SV2B; Lightgreen: GABRA2/5 and GABRG2/3) and genes related to axon and dendrite growth (Table 1; Figures 5B and 5D). Consistent with a role in synaptic function, these modules are also enriched in genes found in biochemically isolated postsynaptic density (PSD) fractions and in genes known to interact with PSD-95 (Bayés et al., 2011) (Table 1; Figure S5D).

We also identified modules related to histone modification and chromatin remodeling (midnightblue) and RNA splicing and processing (red, grey60, and turquoise). The midnightblue module peaks during cortical neurogenesis and contains several members of the chromodomain helicase family (CHD2/3) and the MLL (MLL1/4/5) and BAF (SMARCC2 and SMARCA4) complexes involved in chromatin remodeling, including BAF170/SMARCC2, which was recently implicated in regulation of cortical thickness (Tuoc et al., 2013). Notably, this module also contains transcription factors associated with generation of lower layer neurons, including BCL11B and SOX5, and is expressed early in development when these layers are formed (Molyneaux et al., 2007). The red, grey60, and turquoise modules are also highly expressed early in development, but instead are enriched in genes related to RNA processing and splicing, including several proneural transcription factors (NEUROD1/2/6, NEUROG2; turquoise) and transcription factors expressed in cortical neural progenitors (FEZF2, EMX1; red) and early-generated neurons (TBR1; turquoise). Together, these modules point to critical roles of RNA processing and epigenetic and transcriptional regulation in neural stem cell differentiation during corticogenesis.

Remarkably, we observed that 87% of genes in the network were present in phNPC-conserved modules (17 out of 28 modules; Z score $\geq$ 4) (Figure 5C; Tables 1 and S1) (Langfelder et al., 2011), including all modules related to the major cellular

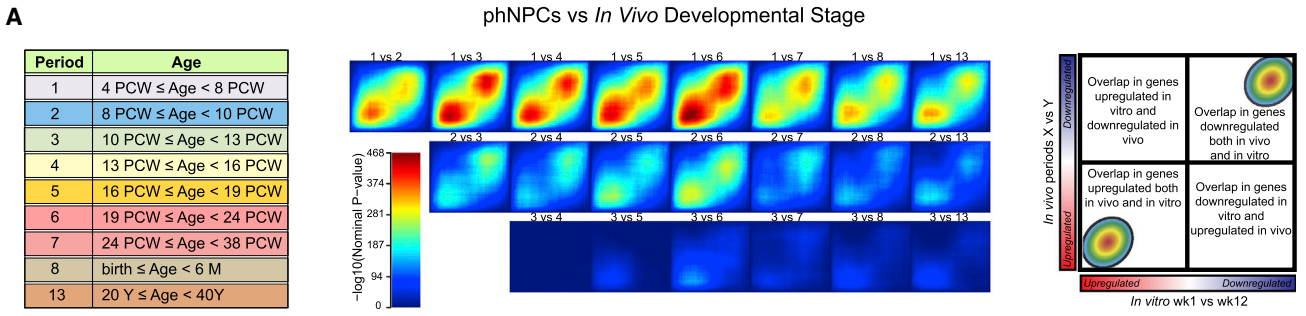

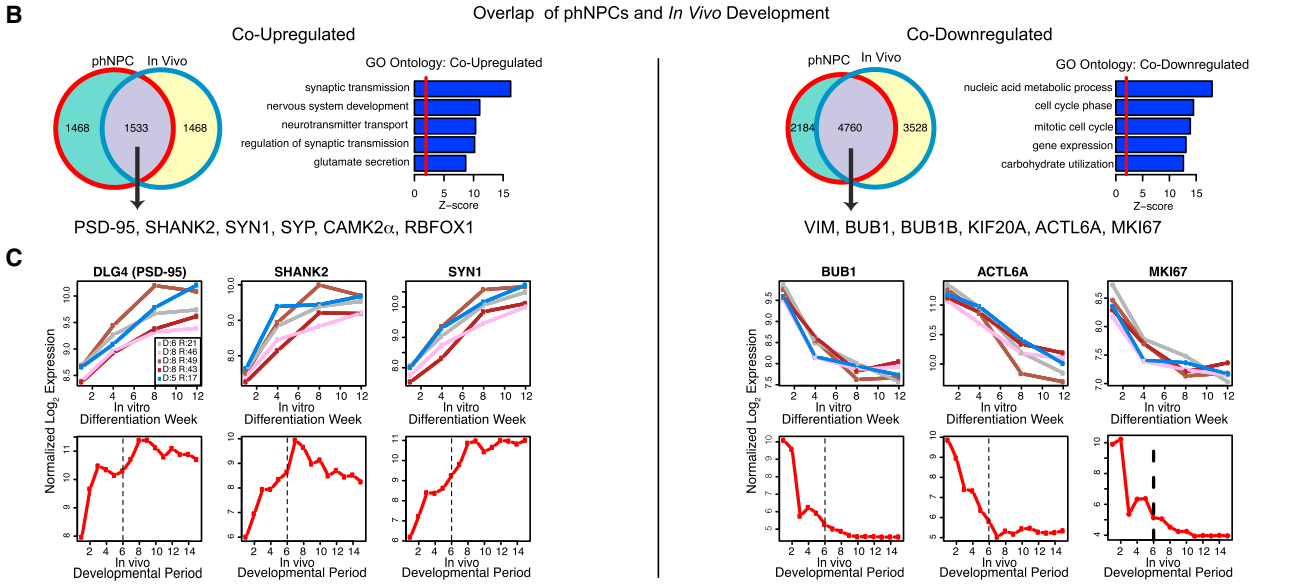

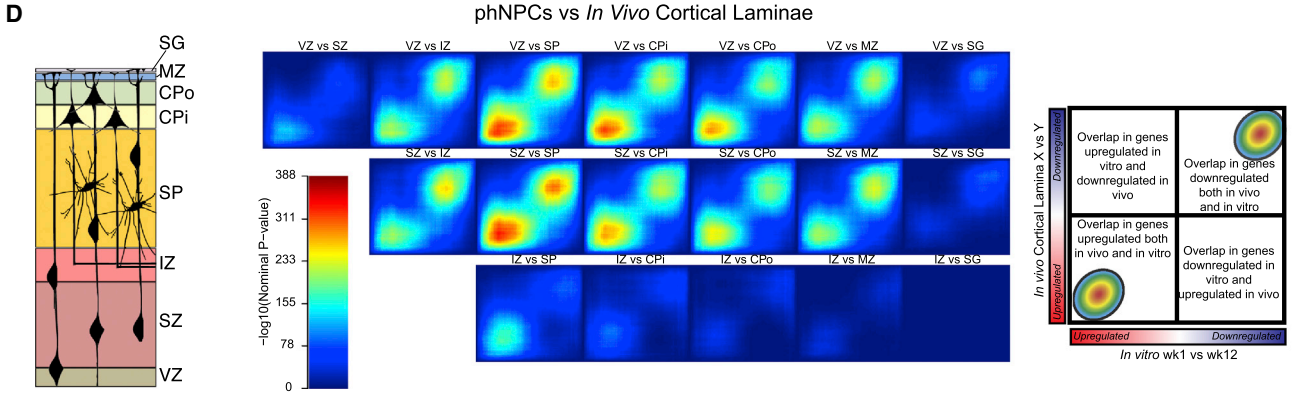

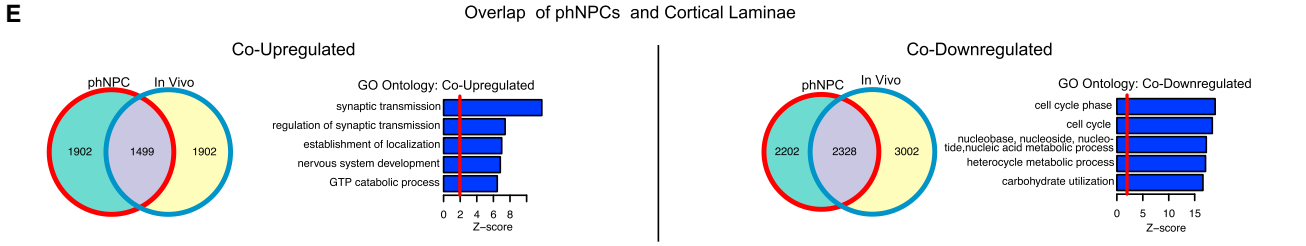

(legend on next page)

and histogenetic processes discussed above. The network architecture of many modules is also strongly preserved, as visually demonstrated by in vivo and in vitro network diagrams (Figures 5D and 5E). Of the modules that were not preserved, two of them are related to immune response (orange and black) and neuron-microglia interactions (orange). This lack of preservation is consistent with the composition of phNPC cultures, which have no detectable microglia (absence of Iba1 staining, data not shown) or immune cells. We also examined module preservation at different time periods in vitro (Figures 5F–5H) and found trends in preservation that are consistent with the module's function—synaptic and gliogenic modules are better preserved at later time points (Figure 5A; Table 1). Half of the modules that were not preserved, including two modules related to vesicle and endosome trafficking, have eigengenes upregulated late in development close to birth, consistent with the mid-fetal maturity of phNPC cultures. Taken together, these parallels in transcriptional network architecture reveal conservation of many biochemical and cellular processes between in vivo fetal brain and in vitro phNPC cultures.

Preserved Modules in phNPCs Are Enriched in ASD Genes

An important question facing the modeling of neurodevelopmental diseases in vitro is to what extent disease-related processes are conserved. Recently, we showed that ASD genes coalesce in several transcriptional modules during fetal human brain development (Parikshak et al., 2013). Similar to Parikshak et al. (2013), we started with a curated list of ASD-associated candidate genes (ASD SFARI) (Banerjee-Basu and Packer, 2010), which showed strong enrichment with the highly preserved in vitro modules related to synaptic function and neurite outgrowth (salmon and yellow; Figure 6A). Importantly, genes coexpressed in ASD and related to synaptic function, previously found to be downregulated in the ASD brain by unbiased transcriptomic analyses (asdM12) (Voineagu et al., 2011), were also enriched in phNPC modules with overlapping function (salmon, skyblue3, lightgreen, green, and purple modules; Figure 6A).

We next tested if rare de novo protein disrupting mutations found in ASD (Iossifov et al., 2012; Neale et al., 2012; O'Roak et al., 2012; Sanders et al., 2012) were similarly enriched in preserved modules. Similar to Parikshak et al. (2013), we found that the conserved phNPC midnightblue module, which contains transcriptional and chromatin regulatory genes, is enriched for these variants (Figure 6A). Remarkably, this module and both synaptic modules are enriched in mRNAs known to interact with FMRP (Figure S5D), suggesting that activity-dependent protein translation dysregulated in ASD can be modeled in vitro. Finally, a group of upregulated genes that is coexpressed in ASD (asdM16; Voineagu et al., 2011) and enriched in astrocyte and microglial markers is enriched in the preserved yellow, pink, tan, magenta, and red modules. As microglia are not observed in the culture, this implies that the astrocyte component of asdM16 shows enrichment in these modules.

Interestingly, genes implicated in other neurodevelopmental diseases including intellectual disability (Inlow and Restifo, 2004; Lubs et al., 2012; Parikshak et al., 2013; Ropers, 2008; van Bokhoven, 2011) and schizophrenia (Levinson et al., 2011) showed enrichment with preserved modules related to basic metabolic cellular processes (ubiquitylation, RNA splicing, and gene expression) and synaptic transmission, respectively (Figure 6A). No enrichment was observed with genes implicated in neurodegenerative disorders, such as late onset Alzheimer's disease (Naj et al., 2011), though this could be due to the relatively small number of genes identified (Figure 6A). Together, these findings suggest that different disorders affect distinct neurodevelopmental processes, many of which can be effectively modeled in vitro using phNPCs.

We further assessed if the coexpression relationships of specific disease-associated genes within our in vivo defined modules were also preserved in vitro. Many ASD-associated genes had generally similar hub status and expression pattern (Figures 6B–6E) in prenatal human cortex and in phNPCs, marking these genes as high-priority candidates for modeling ASD in vitro. These findings link genetic and functional evidence of ASD to known developmental processes that can be modeled in vitro, providing a powerful platform for therapeutic discovery.

Heterogeneity of In Vivo Modeling by Different Human Neural Stem Cell Systems

Advances in stem cell biology in the last decade have facilitated the use of human pluripotent cells, including hES and hiPS cells to study development and disease (Brennand et al., 2011; Kim et al., 2002; Marchetto et al., 2010; Millar et al., 2005; Paşca et al., 2011; Rosen et al., 2011; Ryan et al., 2013; Soldner et al., 2011). However, it is still not known to what degree they recapitulate in vivo development and, most importantly, which specific processes are conserved in which system.

We evaluated the degree of overlap between developing human cortex in vivo and these different systems using the same functional genomics framework developed above. Data sets of differentiating hiPSC (three data sets including one previously published [Paşca et al., 2011] and two unpublished data sets from two separate labs), hESC (Fathi et al., 2011), and

Figure 3. TMAP Identifies In Vivo Developmental Period and Cortical Laminae Most Similar to Differentiating phNPCs

Rank-rank hypergeometric overlap (RRHO) maps (Plaisier et al., 2010) comparing the transitions between in vivo developmental periods ([A]–[C]) or laminae in the developing cortex ([D] and [E]) to differentiation of phNPCs from 1–12 weeks.

(A and D) Each pixel represents the overlap between in vivo and in vitro transcriptome, color-coded according to the $-\log_{10}$ p value of a hypergeometric test (step size = 200). On each map, the extent of shared upregulated genes is displayed in the bottom left corner, whereas shared downregulated genes are displayed in the top right corners (see schematic on rightmost panel).

(B and E) Venn diagrams display the extent of overlap between in vivo and in vitro transcriptomes at the best matched periods (1 versus 6; [B]) and between SZ and CPi (E). Gene ontology (GO Elite) analysis shows coordinately upregulated genes are related to synaptic transmission and nervous system development, whereas codownregulated genes are involved in mitosis.

(C) Selected genes coordinately upregulated and coordinately downregulated are graphed through time both in developing phNPCs and in vivo.

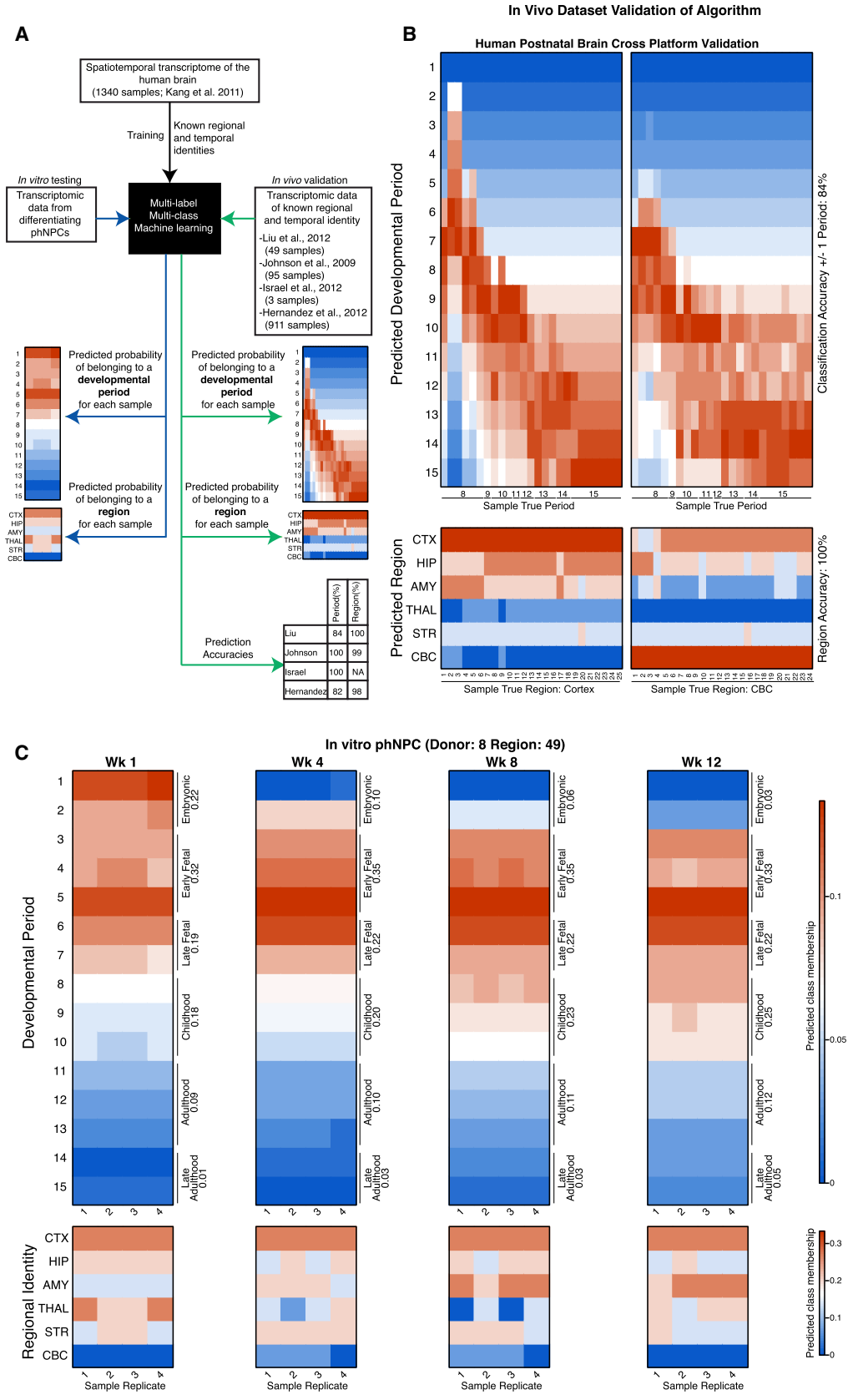

(legend on next page)

Table 1. Summary of High-Confidence Modules Defined in Human Fetal Cortex

Module	In vivo Pzscore	phNPC Pzscore	Select Hub Genes	Biological Processes Associated with Module	ME Time
Magenta	17.0	40.2	BUB1, BUB1B, KIF20A	Mitosis and cell cycle regulation of neural progenitors	
Salmon	14.0	19.9	GRIN1, GRID1, SLC1A1, CAMK2β, VAMP2, SYT3/5	Glutamatergic synaptic transmission, axon and dendrite development	
Cyan	4.1	19.4	NRXN1, PCLO, ANK2/3, MAPT, MYO5A, KIF3B/C, DOCK9	Synapse assembly and vesicle transport by actin/microtubule motors	
Green	28.0	17.6	GABRB1, GRIK4, GRIN3A, SHANK2, RIMS1, SV2B, CACNA1I	Glutamatergic synaptic transmission, axon and dendrite development	
Lightgreen	12.0	15.9	GABRA2/5, GABRG2/3, GLRB, SNAP25, SYT1, SV2A	GABAergic synaptic transmission and synaptic vesicle exocytosis	
Purple	10.0	15.9	SEMA4G, SEMA6C, CRMP1, SRGAP1, DCX	Axon guidance, neuronal migration and GTPase activity	
Red	21.0	14.4	ACTL6A, HIST1H3H, HIST1H2BM, BUB3, CDK4, CNOT1, SRSF1	Mitosis, RNA processing and RNA splicing	
Pink	15.0	7.5	HES1, NOTCH2, FGFR3, RFX4	Neural progenitor proliferation and gliogenesis	
Tan	13.0	5.7	STAT6, TGFBR2/3, CXCL12, CALCRL, TGM2	Reg. of cell death, gliogenesis, immune and inflammatory processes	
Skyblue3	8.8	5.5	SLC17A7, PCDH9, CNTNAP5, ARHGAP44, MGLL	Neuronal, synaptic with parietal areal identity	
Yellow	31.0	5.4	CAMK2A, GRIK1, GFAP, AQP4, CX3CL1	Synaptic transmission, gliogenesis and neuron microglia interaction	
Midnightblue	14.0	5.1	MLL1/4/5, CHD2/3, SMARCA4, CREBBP, FOXG1	Histone modification and chromatin remodeling	
Greenyellow	4.7	4.5	RBFOX1, LUC7L3, CAPRIN2	tRNA processing and RNA binding	
Lightcyan	6.3	4.4	LAMA2/4, COL3A1, COL1A1/2, BMP4, SMAD6	Extracellular matrix and basement membrane, blood vessel development	
Darkred	5.9	4.0	DKK1, BOK, RNF152	Programmed Cell Death	
Grey60	9.8	3.7	THOC1, RBM39, PNN, MRE11A, POLA1, POLE, CNTRL	RNA splicing, DNA repair and cell cyle	
Darkolivegreen	4.5	2.7	COPA, COPE, COPG, VPS11, VAC14, SNAP29	Intracellular protein transport, vesicle and endosome trafficking	
Paleturquoise	5.8	2.3	CACNA2D2, CHRFAM7A, SLC24A2	Synaptic transmission	
Turquoise	15.0	2.3	KLHL9, CRNKL1, CREB1, HDAC2, SENP1	Ubiquitin proteolysis, RNA processing and splicing, reg. gene expression	
Darkgreen	10.0	2.2	ATP6AP1, ATP6V0C, PLEKHB2, DLG4, GOT1, GBA	Endosome and vesicle trafficking, synaptic	
Orange	11.0	1.6	CX3CR1, TYROBP, LAPTM5, CSF1R	Immune response, neuron-microglia interaction	
Darkturquoise	5.0	0.7	NAPA, SORT1, AP2M1, ARF1, MAPK3	Intracellular protein transport, vesicle and endosome trafficking	
Black	12.0	-0.2	BTN3A3, CFB, CTSS, DHX58, HERC5	Immune response	

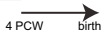

Module preservation Z scores are shown for an independent in vivo dataset of developing human cortex (Colantuoni et al., 2011) and in phNPCs. Modules not preserved in vitro are highlighted in pink with red font, whereas modules preserved in vitro and in vivo are highlighted in green. Select hub genes (from top 100 in each module) related to the biological processes of the module are shown. Modules with few genes (<70) lacking clear or specific GO/KEGG enrichment and no overrepresentation of genes in manually curated lists comprising key neurodevelopmental processes, brain cell populations, and their subcellular compartments (white, steelblue, saddlebrown, yellowgreen, and violet) are preserved in vivo but are not shown in the table. The averaged module eigengene expression from 4 PCW (left) to birth (right) is plotted for each module, represented as a heatmap where red is high and blue is low relative expression.

SY5Y neuroblastoma (Nishida et al., 2008) cells were compared to the human cortex spatiotemporal transcriptome (Kang et al., 2011) (Figure 7A) or the human LCM transcriptome (Miller et al., 2014) (Figure 7B) to map the transitions between developmental periods or cortical laminae in these alternate in vitro systems. These data sets from different laboratories comprise a representative cohort of the differences in culture and differentiation protocols currently available (Supplemental Experimental Procedures). Just as with phNPCs, we found the best overlap in all systems when comparing in vivo period 1 or 2, which contain the germinal zones, to periods of mid-fetal development. As expected, neuroblastoma-derived SY5Y cells had the lowest degree of matching, while hES-derived cells matched relatively well to in vivo cortical development (Figure 7). When differentiated for the same length of time (3 weeks), phNPCs are roughly similar to hES-derived progenitors (Figure S6B). A great degree of heterogeneity of in vivo matching was observed in hiPSCs cultured in different labs using different protocols. Interestingly, hiPSC-derived progenitors from data set 1, even when differentiated longer than hES-derived NPCs or phNPCs, still matched in vivo transcriptional profiles significantly less than phNPCs (Figures S6B and S6C). These differences were not driven by number of samples in the data sets, as hES-derived cells (n = 6) display better matching than hiPSC-derived cells from data set 1 (n = 29) (Supplemental Experimental Procedures). phNPCs from 1 to 8 weeks of differentiation show significantly greater overlap with in vivo development compared to all other in vitro data sets except for hiPSC data set 3, which was roughly equivalent to phNPCs (Figures 3A, 6B, and S6C). hiPSC data set 3 showed strong matching even at 4 weeks of differentiation, implying that it reaches developmental maturity quicker than phNPCs.

TMAP in laminar data (Miller et al., 2014) showed that all systems, except hiPSC data set 3, have significantly less overlap with in vivo laminar transitions than with 8 week PD phNPCs (Figure 3D, 7B, and S6E). Overall, when differentiating for short periods of time, laminar matching is low (Figures S3D and 7B), suggesting that more differentiation in vitro is required to better match in vivo development in most systems. In all systems, more overlap was detected in transitions between proliferative

Figure 4. CoNTExT Predicts Developmental Period and Regional Identity in Individual phNPC Cultures

(A) The CoNTExT algorithm was trained on all samples from a spatio-temporal atlas of human brain expression (Kang et al., 2011) (1,340 samples using Affymetrix Exon 1.0 ST Array) and validated in several postmortem expression data sets. Probability (color in heat map) of each predicted class assignment (y axis) is shown for each sample of known regional and temporal identity (x axis).

(B) Cross platform accuracy was evaluated in 49 samples spanning all postnatal developmental periods and both cerebellar and cortical regions (Liu et al., 2012) (Affymetrix Gene 1.0 ST Array). Developmental period was classified with 84% (±one period) and 100% accuracy in region.

(C) The validated machine learning algorithm was applied to one line (donor: 8; region: 49) of differentiating phNPCs to predict developmental period and regional identity (Illumina HT-12 Beadchip). A clear maturation across differentiation weeks is seen at the individual sample level, with the culture reaching early to late fetal periods of development. In addition, the cultures are predicted to be cortical, consistent with immunocytochemical profile and expression of regional markers.

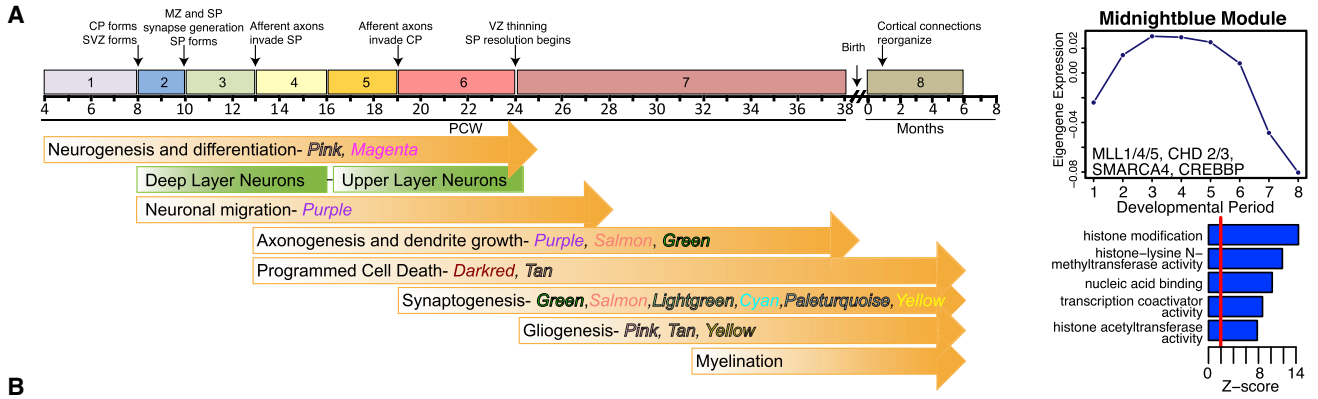

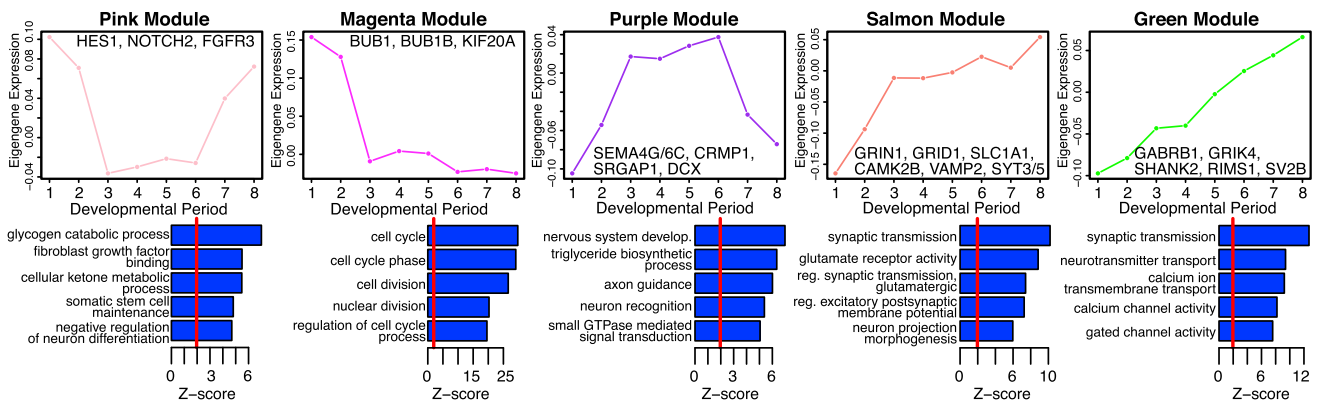

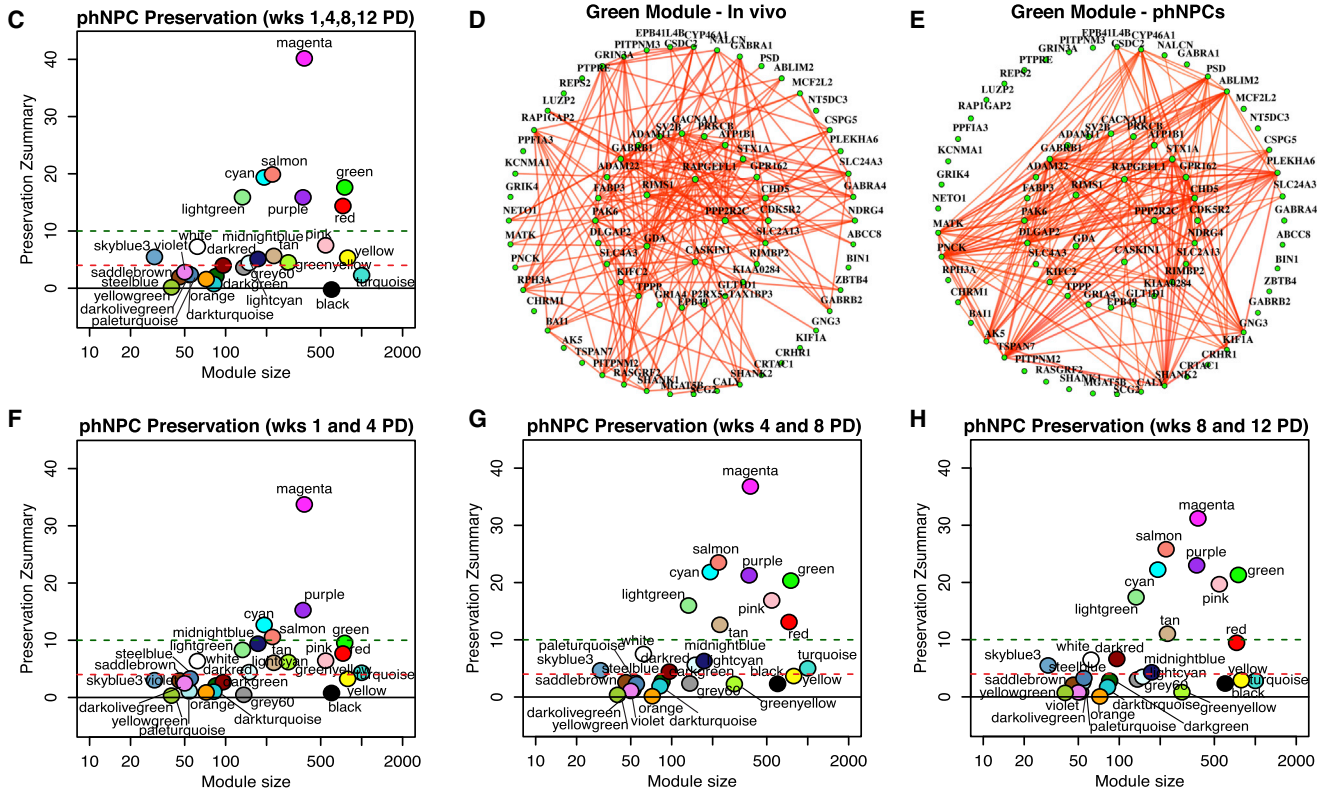

(legend on next page)

layers (VZ and SVZ) and postmitotic layers, consistent with the differentiation of dividing neural progenitors into post mitotic neurons (Figures 3D and 7B).

We next applied CoNTExT to predict individual sample developmental maturity and regional identity (Figure 7C). When CoNTExT predicted a greater difference in culture maturity from progenitor to differentiated cells, stronger in vivo matching was observed in TMAP. This implies that TMAP is mainly measuring similarity to in vivo neural differentiation. This can be seen in hiPSC data set 1 where CoNTExT detected little difference in progenitor versus differentiated cultures, and TMAP showed only a low degree of overlap. CoNTExT was also used to predict regional identity on each individual in vitro sample. Interestingly, several of the hiPSC cultures (data set 1 and 3) showed mixed cortical and cerebellar regional identity. The two samples in data set 3 classified as cortex were derived from the same line and had greater expression of cortical markers and lower expression of caudal markers than other samples from the same data set (data not shown).

To assess which biological processes were preserved in these systems, we applied the WGCNA framework. We first observed poor preservation of network architecture in SY5Y cells. Only the magenta module related to the cessation of proliferation was strongly preserved (Z score > 10), while synaptic modules were weakly preserved or not preserved, consistent with the restricted overlap to downregulated genes in laminar transitions in SY5Y cells (Figures 7D). Across all other in vitro systems (phNPCs, hiPSCs, and hES-derived neural cells), a high degree of preservation (Z > 10) was found for modules relating to neurogenesis and mitosis (magenta and red), neurite outgrowth and synaptogenesis (salmon, lightgreen, and green), and RNA processing and splicing (red). Despite these similarities, differences in developmental processes were apparent across the hiPSC and phNPC systems. The chromatin remodeling midnightblue module (enriched for ASD associated de novo variation; Figure 6), while preserved in phNPCs, was not preserved in the hES and most hiPSC-derived data sets (Figure 7D; this module was preserved in hiPSC data set 2 when subsetting to 1 and 4 weeks PD or 4 and 8 weeks PD; Table S1). Similarly, the pink module related to neural progenitor proliferation and gliogenesis, and the darkred module related to programmed cell death were better or uniquely preserved in phNPCs (Figure 7D). Conversely the turquoise module was better preserved in hiPSC-derived cells. Nonetheless, preservation scores for all highly preserved modules common to all systems were generally higher in phNPCs.

DISCUSSION

Understanding how in vitro systems model in vivo brain development is becoming more important as human neural in vitro systems are becoming more widely used. Benchmarks have long been sought in the stem cell field (Andrews et al., 2005); however, there currently exists no unbiased rubric on which to base such a comparison. We reasoned that transcriptional profiles would provide a comprehensive, unbiased foundation on which to build such a quantitative structure at a genome-wide level. Here, we demonstrate through multiple analytical approaches and validate via multiple independent data sets that phNPCs strongly match in vivo development and produce cortical neurons reaching late mid-fetal levels of maturity after 12 weeks of differentiation. Most, but not all, neurodevelopmental processes of normal corticogenesis are highly preserved in phNPCs. Risk genes for ASD, ID, and schizophrenia are enriched in modules related to these processes. In addition, we find that phNPCs have a stronger overlap and matching with in vivo cortex than other in vitro systems in common use, including some hiPSCs. Furthermore, we identify specific neurodevelopmental processes related to ASD pathophysiology preserved exclusively in phNPCs and not in other in vitro models. Overall, we provide a basic experimental framework for assessing the preservation in vitro of specific biological processes and gene networks underlying cortical development in vivo.

One expectation is that this framework will allow comprehensive evaluation of in vitro systems as they are developed and refined. A variety of protocols exist to generate hiPSCs, including variations in the type of cells used to generate hiPSCs, the standards for characterizing resulting lines, and neural induction and differentiation protocols (Haase et al., 2009; Obokata et al., 2014; Takahashi et al., 2007). Going forward, the comparative framework demonstrated here can be used to optimize protocols to best model in vivo development, including 3D cultures (Kadoshima et al., 2013; Lancaster et al., 2013).

All four parts of our analytic framework are complementary but provide different information. TMAP provides a global view of transcriptomic matching to in vivo development. TMAP is mainly driven by differentiation processes that are not regionally specific, so it should not be considered a regional identity tool. Using human in vivo cerebellar or striatal data as input to TMAP, for example, still shows a high degree of in vitro matching with the cortical phNPCs (data not shown). CoNTExT is a useful framework for individual sample prediction of temporal and regional

Figure 5. Network Analysis Identifies Major Neurodevelopmental Processes that Are Preserved in Differentiating phNPCs

(A) A weighted gene coexpression network was formed using human cortex samples from embryonic (Period 1) to neonatal periods (Period 8). Timeline of known cellular and histogenetic processes in the developing human brain (Andersen, 2003; Kang et al., 2011) and modules enriched in genes related these processes are labeled.

(B) A subset of modules related to key neurodevelopmental processes are highlighted with corresponding GO analysis, selected hub genes, and module eigengene trajectories (see Table 1 for full list).

(C) Module preservation (Langfelder et al., 2011) in phNPCs differentiated over 12 weeks shows high preservation (Z ≥ 4) of 12 modules.

(D and E) The green module, enriched in genes involved in synaptic function, shows a similar pattern of connectivity in vivo (D) and in vitro (E). The width and color of the edges are weighted by the strength of bicorrelation.

(F–H) Module preservation varies over differentiation time. Early differentiation periods (F) show stronger preservation of chromatin modification genes (midnightblue module) while later time periods ([G] and [H]) show stronger preservation of gliogenic (pink and tan modules) and synaptogenic (salmon, green, lightgreen, and cyan modules) genes.

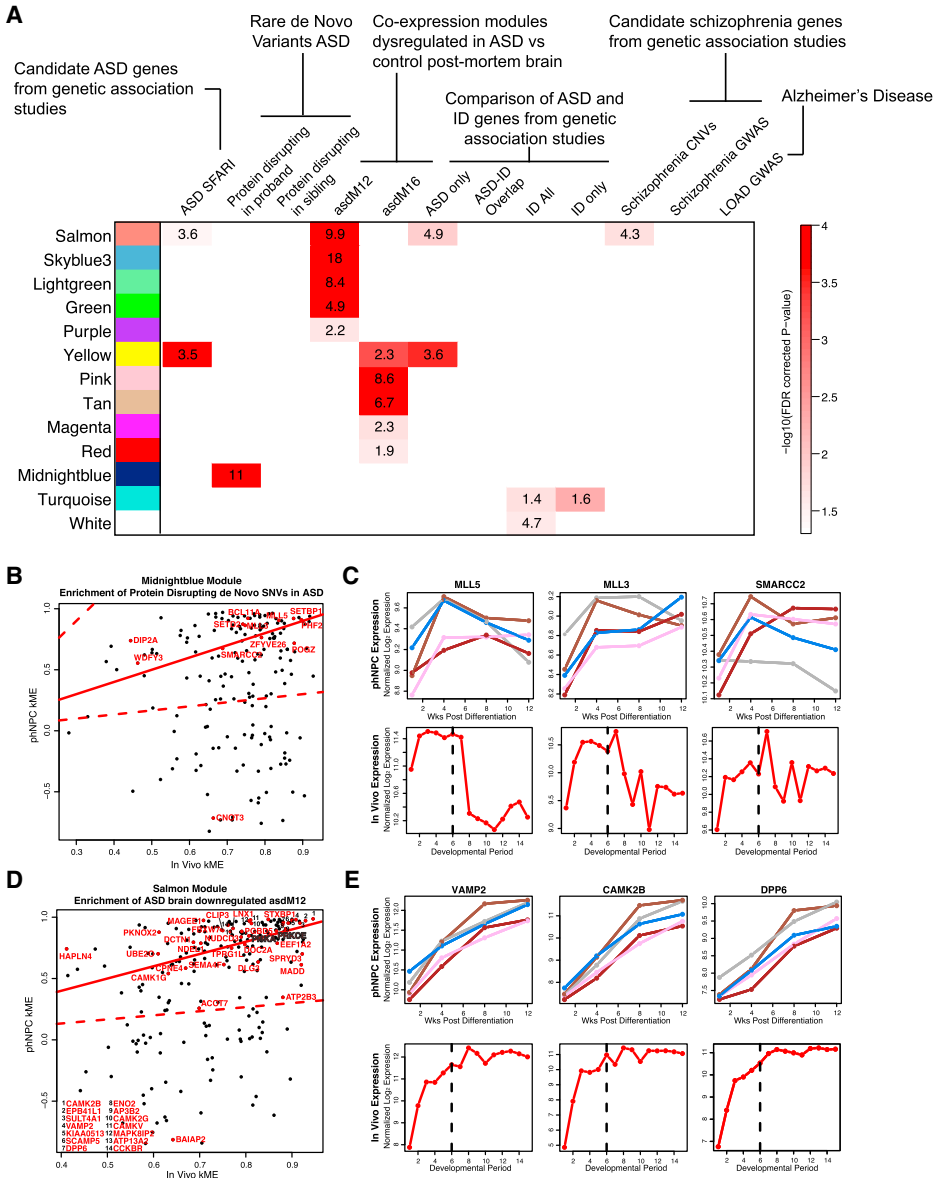

Figure 6. phNPC Preserved Modules Are Enriched in ASD-Associated Genes

(A) In-vivo-defined modules preserved in differentiating phNPCs were tested for enrichment of disease-associated genes from a curated list of autism-associated genes (ASD SFARI) (Banerjee-Basu and Packer, 2010), rare de novo protein disrupting mutations found in ASD and siblings (Iossifov et al., 2012; Neale et al., 2012; O'Roak et al., 2012; Sanders et al., 2012), two ASD-associated modules defined in postmortem brain (asdM12 and asdM16) (Voineagu et al., 2011), a curated list of genes associated with intellectual disability (ID All) (Inlow and Restifo, 2004; Lubs et al., 2012; Parikshak et al., 2013; Ropers, 2008; van Bokhoven, 2011), the intersection of ASD SFARI with ID (ASD-ID overlap), the relative complement of these (ASD only; ID only), a list of genes disrupted by CNVs in schizophrenia (Levinson et al., 2011), genes near significantly associated loci in GWAS of schizophrenia (Ripke et al., 2013), and genes near significantly associated loci in GWAS of late onset Alzheimer's disease (Naj et al., 2011). Enrichment was assessed using Fisher's exact test, and the FDR (Benjamini and Hochberg, 1995) correction for multiple comparisons p value is displayed.

(B) Protein disrupting de novo SNVs found in ASD are enriched in the preserved midnightblue module. The correlation of each gene to the module eigengene (kME) is shown for in vivo and phNPC data (1 and 4 week PD). ASD-associated genes are highlighted in red. Genes close to the solid red line (y = x) have the same kME in vivo and in vitro. The dotted red line represents an in vivo kME value three times less than observed in vivo.

(C) Several genes that contain ASD-associated de novo SNVs have similar expression patterns in vivo and in vitro.

(D) kME is shown for in vivo and phNPC data (1, 4, 8, and 12 week PD) for the preserved salmon module that is enriched in asdM12 genes (Voineagu et al., 2011). ASD-associated genes in asdM12 are in red and are labeled.

(E) Several asdM12 genes show similar expression patterns in vivo and in vitro.

identity. One caveat to its use is that the algorithm must classify a sample into one of the defined regions or time periods, even if it matches none of them. As such, we defined through simulation how the level of in vivo matching affects the accuracy of classification (Figures S4D and S4E). Finally, CoNTExT and TMAP do not specify which molecular pathways are conserved. WGCNA module preservation is a well-validated tool to determine the specific functional processes that are preserved in vitro. For those processes not conserved, modifying the expression of key hub genes in the module using exogenous factors like small molecules or by targeted gene expression may provide leverage for developing more faithful in vivo modeling in the future.

The observed differences between in vitro systems could be due to inherent properties of the system, reprogramming, culture conditions, or even culturing technique. While with the current data we cannot pinpoint the source of variance, it is interesting to note that hiPSC data sets generated using more recent protocols, which include addition of morphogens (SMAD inhibitors) for neural induction, match better to in vivo brain. Similarly, because the time spent in the neural induction stage differs between systems, the initial (NPC) time point may reflect different starting points of maturity. Nonetheless, significant heterogeneity exists even within hiPSCs cultured in identical conditions. In the highest in vivo matching hiPSC data set by TMAP, we observed one clone with strongly different regional identity compared to another clone derived from the same donor (Figure 7; data set 3). The in vivo transcriptomic framework provided here can be used to systemically test how these and other factors can optimize matching to in vivo developmental transitions or regional identify.

Differences between pluripotent-derived and primary neural progenitors have been identified in previous studies, including low or undetectable expression of the radial glia marker GFAP and overall higher production of neurons upon differentiation (Falk et al., 2012). GFAP is expressed in radial glia in vivo (Wilkinson et al., 1990) and in undifferentiated phNPCs, and its absence in hiPSC-derived progenitors may be related to their more immature neuroepithelial nature (Falk et al., 2012).

Growing evidence implicates abnormalities in the development and architecture of the human cerebral cortex in neuropsychiatric illness (Akbarian et al., 1996; Anderson et al., 1996; Ebert and Greenberg, 2013; Gulsuner et al., 2013; Hutsler and Zhang, 2010; Parikshak et al., 2013; Penzes et al., 2011; Strauss et al., 2006; Wegiel et al., 2012; Willsey et al., 2013). We identified a module related to chromatin remodeling (midnightblue) that is largely not preserved in hiPS-derived neural stem cells and contains key genes involved in the generation of lower layer neurons and that regulate cortical thickness in rodent (Tuoc et al., 2013). Chromatin remodeling and transcriptional regulation are key biological processes that are enriched for protein disrupting and missense rare de novo mutations in ASD (Parikshak et al., 2013). These findings underscore critical differences in widely used in vitro systems that may compromise their utility for the study of development and neuropsychiatric disease. At the same time, because they can be derived from well-characterized patients and carry their full genetic background, hiPSC-derived NPCs have clear value. Our approach provides a template to refine these systems to better match in vivo brain development.

In this regard, our analysis also highlights processes poorly preserved in all of the vitro models, including modules related to immune response and neuron-microglia interactions (orange and black). A hub in the orange module, CX3CR1, is specifically expressed in microglia and mediates neuron-microglia signaling implicated in regulating neuronal death during neuroinflammation (Cardona et al., 2006; Fuhrmann et al., 2010). The neuronal ligand of CX3CR1, the fractalkine CX3CL1, is in the weakly preserved neuronal yellow module; this signaling pair regulates developmental synaptic pruning (Paolicelli et al., 2011). Given the emerging role for microglia in neurodevelopmental and neurodegenerative diseases (Paolicelli et al., 2011; Vargas et al., 2005), it will be important to evaluate if addition of microglia to differentiating phNPCs will be sufficient to recapitulate these processes.

These results also stress that current human neural stem cell systems, including hiPSCs, represent an immature, fetal state, consistent with other published work (Brennand et al., 2014; Espuny-Camacho et al., 2013; Kadoshima et al., 2013; Mariani et al., 2012; Nicholas et al., 2013). This is a key issue that may present challenges for modeling late-onset brain disorders including Alzheimer's disease. It will be important to evaluate to what extent phenotypes in these immature neurons can be translated effectively into relevant pathophysiological insights (Sandoe and Eggan, 2013). Transcriptomic data can be leveraged to identify key processes and genes that may drive the generation of specific populations of cells or a desired level of maturity.

The methods presented here represent a first step in determining the degree of matching of in vitro systems to in vivo development. We realize that the ultimate understanding of how well in vitro cultures match in vivo development will be from matching individual cell transcriptomes from different regions, laminae, and developmental time periods to individual cell transcriptomes grown in culture. Importantly, in the future as comprehensive data sets of additional genomic data across cell populations in the developing brain become available, our approach can integrate different data modalities to provide a robust picture of the matching of neural stem cell models to in vivo brain. This approach can also provide mechanistic insight into differences between systems, which can be leveraged to improve the fidelity of in vitro models. This is especially important if our goal is to understand and develop treatments for human disease.

EXPERIMENTAL PROCEDURES

Tissue Acquisition and Cell Culture

Human fetal brain tissue was obtained from the UCLA Gene and Cell Therapy Core following IRB regulations. phNPC cultures were prepared from PCW 15–18 human fetal brain as described (Konopka et al., 2012; Wexler et al., 2011) and detailed in Supplemental Experimental Procedures.

Genotyping

DNA was acquired from phNPCs cultures or fetal brain tissue and donors were genotyped with Illumina HumanOmni2.5 chips. Sex was determined based on homozygosity in X chromosome SNPs (two male; one female). High confidence CNVs called with CNVision (Sanders et al., 2011) were not found in autism-associated regions.

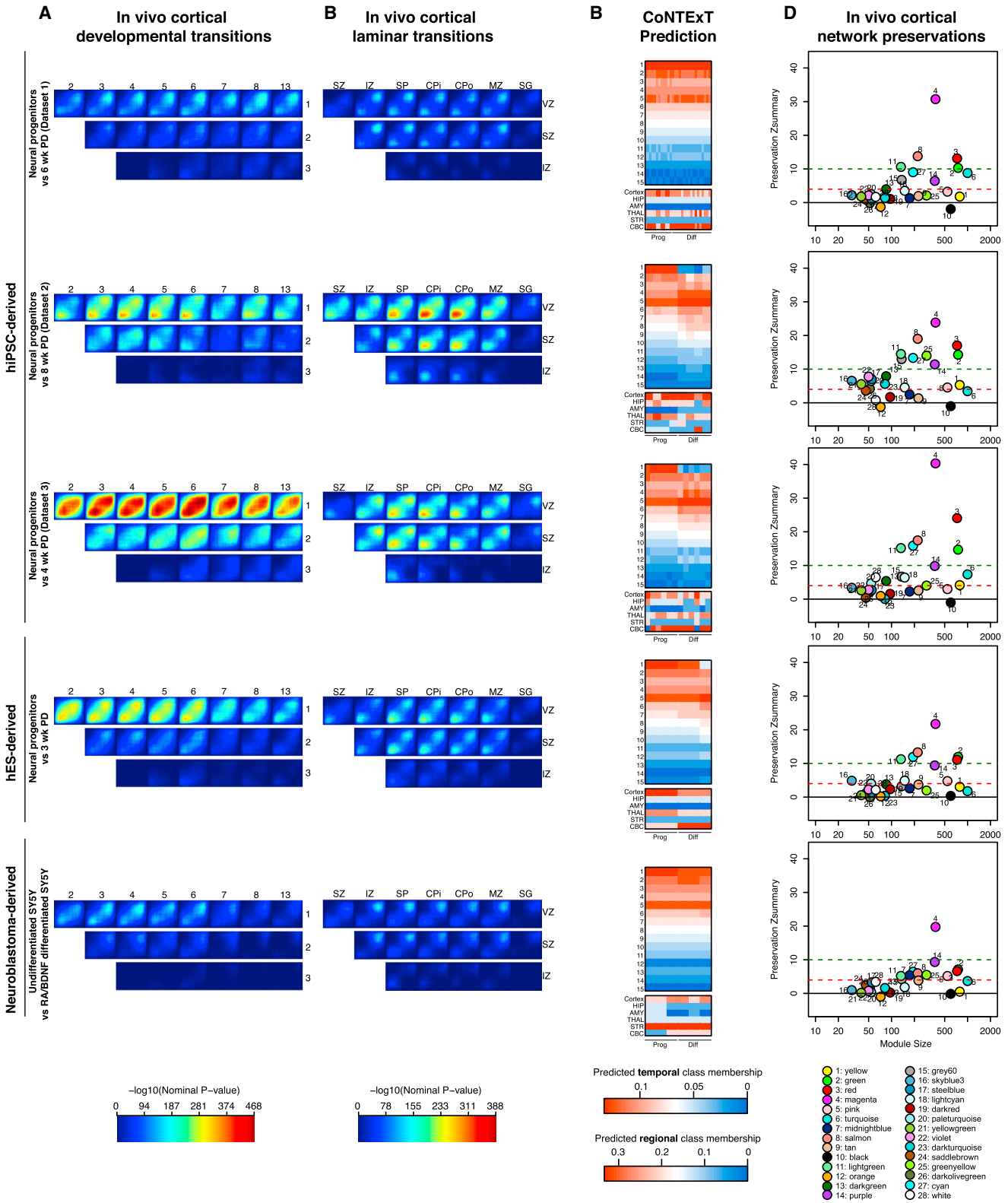

Figure 7. The Extent of In Vivo Overlap Observed in Multiple In Vitro Neural Stem Cell Models

(A and B) The transitions between in vivo developmental periods of neocortex (Kang et al., 2011) (A) or laminae in the developing cortex (Miller et al., 2014) (B) are compared to the transition between proliferative and differentiated neuronal cultures derived from thre data sets of hiPSC cells, hES (Fathi et al., 2011), and SY5Y

(legend continued on next page)

Immunocytochemistry

Immunostaining was performed on PFA fixed cells with the indicated antibodies and the DNA-binding dye 4′,6-diamidino-2-phenylindole (DAPI) to quantify total cell number and cell viability. Detailed protocol and a list of antibodies used in this study is provided in Supplemental Experimental Procedures. Images were captured using a Zeiss Axio Imager D1 (Thornwood) epifluorescence microscope and analyzed using ImageJ software.

RNA Isolation, Processing, and Microarray Hybridization

For each of 5 lines generated from three donors (15–16 PCW), two independent differentiation experiments each containing two replicates were performed and harvested at four time points (1, 4, 8, and 12 weeks PD; ~16 samples per line; 77 total samples). RNA was isolated using TRIzol reagent (Invitrogen) according to standard protocols. We confirmed RNA integrity by RIN score with the Agilent 2100 Bioanalyzer (mean ± SD: 9.16 ± 0.78). Further details are found in Supplemental Experimental Procedures. All RNA expression profiles acquired as part of this project are publicly available (GSE57595).

TMAP

A spatiotemporal atlas of human brain gene expression (Kang et al., 2011) and laminar expression data dissected via Laser Capture Microdissection from fetal human brain (Miller et al., 2014) were downloaded. For TMAP, differential expression between time points was calculated using a mixed effects model implemented in the nlme package (Pinheiro and Bates, 2009), with a random effect representing cell line (in vitro) or donor (in vivo), to appropriately account for the repeated-measures of multiple nonindependent samples (replicates of lines in phNPCs; multiple regions from the same donor in vivo). The rank-rank hypergeometric overlap test (Plaisier et al., 2010) was implemented using custom R scripts now available as a Bioconductor package (RRHO) to evaluate overlap between in vivo and in vitro data sets. Further details are found in Supplemental Experimental Procedures.

CoNTExT

A multiclass, multilabel machine learning algorithm was implemented in the MEKA toolbox (http://meka.sourceforge.net/) (Read, 2010) and trained on all 1,340 samples of the Kang et al., 2011 data using all regions and all time points. Classification accuracy of developmental period was evaluated for each downloaded data set within a range of ±1 from the true value to account for edge effects and ambiguities in the determination of conception date. For each sample, the probability of belonging to each class was output and displayed in Figures 4 and S4. A simulation was conducted to judge the accuracy of the classifier at different levels on in vivo matching Figure S4. Further details are found in Supplemental Experimental Procedures.

WGCNA

WGCNA was conducted using the R package WGCNA (Langfelder and Horvath, 2008) on the neocortical samples from Kang et al. (2011) data set from time periods 1 through 8. Module preservation analysis was conducted to determine if density and connectivity-based measures were preserved in vitro (Langfelder et al., 2011). Further details are found in Supplemental Experimental Procedures.

GO Ontologies

GO analysis was completed using GO-Elite v1.2.5 with default settings (Zambon et al., 2012). Relevant biological process and molecular function categories were plotted selected from the top 10 terms ranked by Z score.

SUPPLEMENTAL INFORMATION

Supplemental Information includes six figures, one table, and Supplemental Experimental Procedures and can be found with this article online at http://dx.doi.org/10.1016/j.neuron.2014.05.035.

AUTHOR CONTRIBUTIONS

J.L.S., L.T.U., and D.H.G. conceived and designed the experiments and wrote the manuscript. A.R.M., K.S.K., F.H.G, I.A.H., M.C.M., and C.R.H. provided iPSCs and iPSC-derived neuronal lines. E.M.W. helped develop phNPC protocols. N.N.P., Y.T. J.K.L., and D.K.B. contributed to analysis. D.L. cultured cell lines and extracted RNA.

ACKNOWLEDGMENTS

Fetal tissue was acquired in collaboration with CFAR grant 5P30 AI028697. Expression and genotype array data were generated by the UCLA Neuroscience Genomics Core. This work was supported by NIH grants to D.H.G. (5R37 MH060233; 5R01 MH094714), J.L.S. (K99MH102357), and L.T.U. (T32MH073526); the Broad Stem Cell Research Center (BSCRC) (D.H.G., J.L.S., and L.T.U.); Autism Speaks (J.L.S.); the California Institute for Regenerative Medicine (CIRM)-BSCRC Training Grant (TG2-01169)-(L.T.U.); and the Dr. Miriam and Sheldon Adelson Medical Foundation (K.S.K.). We thank Yadong Huang and Hyung-Seok Kim for assistance with reprogramming of patient fibroblasts. We thank Yining Zhao for website development. We thank members of the Geschwind laboratory for helpful discussions and critical reading of the manuscript.

Accepted: May 21, 2014
Published: July 2, 2014

REFERENCES

Akbarian, S., Kim, J.J., Potkin, S.G., Hetrick, W.P., Bunney, W.E., Jr., and Jones, E.G. (1996). Maldistribution of interstitial neurons in prefrontal white matter of the brains of schizophrenic patients. Arch. Gen. Psychiatry *53*, 425–436.

An, M.C., Zhang, N., Scott, G., Montoro, D., Wittkop, T., Mooney, S., Melov, S., and Ellerby, L.M. (2012). Genetic correction of Huntington's disease phenotypes in induced pluripotent stem cells. Cell Stem Cell *11*, 253–263.

Andersen, S.L. (2003). Trajectories of brain development: point of vulnerability or window of opportunity? Neurosci. Biobehav. Rev. *27*, 3–18.

Anderson, S.A., Volk, D.W., and Lewis, D.A. (1996). Increased density of microtubule associated protein 2-immunoreactive neurons in the prefrontal white matter of schizophrenic subjects. Schizophr. Res. *19*, 111–119.

Andrews, P.W., Benvenisty, N., McKay, R., Pera, M.F., Rossant, J., Semb, H., and Stacey, G.N.; Steering Committee of the International Stem Cell Initiative (2005). The International Stem Cell Initiative: toward benchmarks for human embryonic stem cell research. Nat. Biotechnol. *23*, 795–797.

Arlotta, P., Molyneaux, B.J., Chen, J., Inoue, J., Kominami, R., and Macklis, J.D. (2005). Neuronal subtype-specific genes that control corticospinal motor neuron development in vivo. Neuron *45*, 207–221.

Banerjee-Basu, S., and Packer, A. (2010). SFARI Gene: an evolving database for the autism research community. Dis. Model. Mech. *3*, 133–135.

neuroblastoma (Nishida et al., 2008) cells. The color bars are on the same scale as Figure 3. Comparisons of in vivo overlap between in vitro systems are found in Figure S6.

(C) The machine learning framework CoNTExT was used to predict the regional and temporal identity of each sample. The identity of each sample as progenitor or differentiated is labeled below the heatmaps. The accuracy of CoNTExT predictions is related to the degree of in vitro matching, so low matching systems may not have accurate predictions (Figure S4).

(D) Module preservation was used to test which processes were conserved in different in vivo systems on the same scale as Figure 5.

Bayés, A., van de Lagemaat, L.N., Collins, M.O., Croning, M.D., Whittle, I.R., Choudhary, J.S., and Grant, S.G. (2011). Characterization of the proteome, diseases and evolution of the human postsynaptic density. Nat. Neurosci. *14*, 19–21.

Benjamini, Y., and Hochberg, Y. (1995). Controlling the False Discovery Rate - a Practical and Powerful Approach to Multiple Testing. J. Roy. Sta.t Soc. B. Met. *57*, 289–300.

Betizeau, M., Cortay, V., Patti, D., Pfister, S., Gautier, E., Bellemin-Ménard, A., Afanassieff, M., Huissoud, C., Douglas, R.J., Kennedy, H., and Dehay, C. (2013). Precursor diversity and complexity of lineage relationships in the outer subventricular zone of the primate. Neuron *80*, 442–457.

Brennand, K.J., Simone, A., Jou, J., Gelboin-Burkhart, C., Tran, N., Sangar, S., Li, Y., Mu, Y., Chen, G., Yu, D., et al. (2011). Modelling schizophrenia using human induced pluripotent stem cells. Nature *473*, 221–225.

Brennand, K., Savas, J.N., Kim, Y., Tran, N., Simone, A., Hashimoto-Torii, K., Beaumont, K.G., Kim, H.J., Topol, A., Ladran, I., et al. (2014). Phenotypic differences in hiPSC NPCs derived from patients with schizophrenia. Mol. Psychiatry. http://dx.doi.org/10.1038/mp.2014.22.

Cardona, A.E., Pioro, E.P., Sasse, M.E., Kostenko, V., Cardona, S.M., Dijkstra, I.M., Huang, D., Kidd, G., Dombrowski, S., Dutta, R., et al. (2006). Control of microglial neurotoxicity by the fractalkine receptor. Nat. Neurosci. *9*, 917–924.

Colantuoni, C., Lipska, B.K., Ye, T., Hyde, T.M., Tao, R., Leek, J.T., Colantuoni, E.A., Elkahloun, A.G., Herman, M.M., Weinberger, D.R., and Kleinman, J.E. (2011). Temporal dynamics and genetic control of transcription in the human prefrontal cortex. Nature *478*, 519–523.

Dolmetsch, R., and Geschwind, D.H. (2011). The human brain in a dish: the promise of iPSC-derived neurons. Cell *145*, 831–834.

Ebert, D.H., and Greenberg, M.E. (2013). Activity-dependent neuronal signalling and autism spectrum disorder. Nature *493*, 327–337.

Englund, C., Fink, A., Lau, C., Pham, D., Daza, R.A., Bulfone, A., Kowalczyk, T., and Hevner, R.F. (2005). Pax6, Tbr2, and Tbr1 are expressed sequentially by radial glia, intermediate progenitor cells, and postmitotic neurons in developing neocortex. J. Neurosci. *25*, 247–251.

Espuny-Camacho, I., Michelsen, K.A., Gall, D., Linaro, D., Hasche, A., Bonnefont, J., Bali, C., Orduz, D., Bilheu, A., Herpoel, A., et al. (2013). Pyramidal neurons derived from human pluripotent stem cells integrate efficiently into mouse brain circuits in vivo. Neuron *77*, 440–456.

Falk, A., Koch, P., Kesavan, J., Takashima, Y., Ladewig, J., Alexander, M., Wiskow, O., Tailor, J., Trotter, M., Pollard, S., et al. (2012). Capture of neuroepithelial-like stem cells from pluripotent stem cells provides a versatile system for in vitro production of human neurons. PLoS ONE *7*, e29597.

Fathi, A., Hatami, M., Hajihosseini, V., Fattahi, F., Kiani, S., Baharvand, H., and Salekdeh, G.H. (2011). Comprehensive gene expression analysis of human embryonic stem cells during differentiation into neural cells. PLoS ONE *6*, e22856.

Fietz, S.A., Kelava, I., Vogt, J., Wilsch-Brauninger, M., Stenzel, D., Fish, J.L., Corbeil, D., Riehn, A., Distler, W., Nitsch, R., et al. (2010). OSVZ progenitors of human and ferret neocortex are epithelial-like and expand by integrin signaling. Nat. Neurosci. *13*, 690–699.

Fuhrmann, M., Bittner, T., Jung, C.K., Burgold, S., Page, R.M., Mitteregger, G., Haass, C., LaFerla, F.M., Kretzschmar, H., and Herms, J. (2010). Microglial Cx3cr1 knockout prevents neuron loss in a mouse model of Alzheimer's disease. Nat. Neurosci. *13*, 411–413.

Gleeson, J.G., Lin, P.T., Flanagan, L.A., and Walsh, C.A. (1999). Doublecortin is a microtubule-associated protein and is expressed widely by migrating neurons. Neuron *23*, 257–271.

Goshima, Y., Nakamura, F., Strittmatter, P., and Strittmatter, S.M. (1995). Collapsin-induced growth cone collapse mediated by an intracellular protein related to UNC-33. Nature *376*, 509–514.

Gulsuner, S., Walsh, T., Watts, A.C., Lee, M.K., Thornton, A.M., Casadei, S., Rippey, C., Shahin, H., Nimgaonkar, V.L., Go, R.C., et al.; Consortium on the Genetics of Schizophrenia (COGS); PAARTNERS Study Group (2013). Spatial and temporal mapping of de novo mutations in schizophrenia to a fetal prefrontal cortical network. Cell *154*, 518–529.

Haase, A., Olmer, R., Schwanke, K., Wunderlich, S., Merkert, S., Hess, C., Zweigerdt, R., Gruh, I., Meyer, J., Wagner, S., et al. (2009). Generation of induced pluripotent stem cells from human cord blood. Cell Stem Cell *5*, 434–441.

Hansen, D.V., Lui, J.H., Parker, P.R., and Kriegstein, A.R. (2010). Neurogenic radial glia in the outer subventricular zone of human neocortex. Nature *464*, 554–561.

Hansen, D.V., Rubenstein, J.L., and Kriegstein, A.R. (2011). Deriving excitatory neurons of the neocortex from pluripotent stem cells. Neuron *70*, 645–660.

Hawrylycz, M.J., Lein, E.S., Guillozet-Bongaarts, A.L., Shen, E.H., Ng, L., Miller, J.A., van de Lagemaat, L.N., Smith, K.A., Ebbert, A., Riley, Z.L., et al. (2012). An anatomically comprehensive atlas of the adult human brain transcriptome. Nature *489*, 391–399.

Hernandez, D.G., Nalls, M.A., Moore, M., Chong, S., Dillman, A., Trabzuni, D., Gibbs, J.R., Ryten, M., Arepalli, S., Weale, M.E., et al. (2012). Integration of GWAS SNPs and tissue specific expression profiling reveal discrete eQTLs for human traits in blood and brain. Neurobiol. Dis. *47*, 20–28.

Hutsler, J.J., and Zhang, H. (2010). Increased dendritic spine densities on cortical projection neurons in autism spectrum disorders. Brain Res. *1309*, 83–94.

Inlow, J.K., and Restifo, L.L. (2004). Molecular and comparative genetics of mental retardation. Genetics *166*, 835–881.

Iossifov, I., Ronemus, M., Levy, D., Wang, Z., Hakker, I., Rosenbaum, J., Yamrom, B., Lee, Y.H., Narzisi, G., Leotta, A., et al. (2012). De novo gene disruptions in children on the autistic spectrum. Neuron *74*, 285–299.

Israel, M.A., Yuan, S.H., Bardy, C., Reyna, S.M., Mu, Y., Herrera, C., Hefferan, M.P., Van Gorp, S., Nazor, K.L., Boscolo, F.S., et al. (2012). Probing sporadic and familial Alzheimer's disease using induced pluripotent stem cells. Nature *482*, 216–220.

Johnson, M.B., Kawasawa, Y.I., Mason, C.E., Krsnik, Z., Coppola, G., Bogdanović, D., Geschwind, D.H., Mane, S.M., State, M.W., and Sestan, N. (2009). Functional and evolutionary insights into human brain development through global transcriptome analysis. Neuron *62*, 494–509.

Kadoshima, T., Sakaguchi, H., Nakano, T., Soen, M., Ando, S., Eiraku, M., and Sasai, Y. (2013). Self-organization of axial polarity, inside-out layer pattern, and species-specific progenitor dynamics in human ES cell-derived neocortex. Proc. Natl. Acad. Sci. USA *110*, 20284–20289.

Kageyama, R., Ohtsuka, T., Shimojo, H., and Imayoshi, I. (2008). Dynamic Notch signaling in neural progenitor cells and a revised view of lateral inhibition. Nat. Neurosci. *11*, 1247–1251.

Kang, H.J., Kawasawa, Y.I., Cheng, F., Zhu, Y., Xu, X., Li, M., Sousa, A.M., Pletikos, M., Meyer, K.A., Sedmak, G., et al. (2011). Spatio-temporal transcriptome of the human brain. Nature *478*, 483–489.

Kang, P., Lee, H.K., Glasgow, S.M., Finley, M., Donti, T., Gaber, Z.B., Graham, B.H., Foster, A.E., Novitch, B.G., Gronostajski, R.M., and Deneen, B. (2012). Sox9 and NFIA coordinate a transcriptional regulatory cascade during the initiation of gliogenesis. Neuron *74*, 79–94.

Kim, J.H., Auerbach, J.M., Rodríguez-Gómez, J.A., Velasco, I., Gavin, D., Lumelsky, N., Lee, S.H., Nguyen, J., Sánchez-Pernaute, R., Bankiewicz, K., and McKay, R. (2002). Dopamine neurons derived from embryonic stem cells function in an animal model of Parkinson's disease. Nature *418*, 50–56.

Konopka, G., Wexler, E., Rosen, E., Mukamel, Z., Osborn, G.E., Chen, L., Lu, D., Gao, F., Gao, K., Lowe, J.K., and Geschwind, D.H. (2012). Modeling the functional genomics of autism using human neurons. Mol. Psychiatry *17*, 202–214.

Kriegstein, A., and Alvarez-Buylla, A. (2009). The glial nature of embryonic and adult neural stem cells. Annu. Rev. Neurosci. *32*, 149–184.

Lancaster, M.A., Renner, M., Martin, C.A., Wenzel, D., Bicknell, L.S., Hurles, M.E., Homfray, T., Penninger, J.M., Jackson, A.P., and Knoblich, J.A. (2013). Cerebral organoids model human brain development and microcephaly. Nature *501*, 373–379.

Langfelder, P., and Horvath, S. (2008). WGCNA: an R package for weighted correlation network analysis. BMC Bioinformatics *9*, 559.

Langfelder, P., Luo, R., Oldham, M.C., and Horvath, S. (2011). Is my network module preserved and reproducible? PLoS Comput. Biol. *7*, e1001057.

Levinson, D.F., Duan, J., Oh, S., Wang, K., Sanders, A.R., Shi, J., Zhang, N., Mowry, B.J., Olincy, A., Amin, F., et al. (2011). Copy number variants in schizophrenia: confirmation of five previous findings and new evidence for 3q29 microdeletions and VIPR2 duplications. Am. J. Psychiatry *168*, 302–316.

Liu, X., Somel, M., Tang, L., Yan, Z., Jiang, X., Guo, S., Yuan, Y., He, L., Oleksiak, A., Zhang, Y., et al. (2012). Extension of cortical synaptic development distinguishes humans from chimpanzees and macaques. Genome Res. *22*, 611–622.

Lubs, H.A., Stevenson, R.E., and Schwartz, C.E. (2012). Fragile X and X-linked intellectual disability: four decades of discovery. Am. J. Hum. Genet. *90*, 579–590.

Manuel, M., and Price, D.J. (2005). Role of Pax6 in forebrain regionalization. Brain Res. Bull. *66*, 387–393.

Marchetto, M.C., Carromeu, C., Acab, A., Yu, D., Yeo, G.W., Mu, Y., Chen, G., Gage, F.H., and Muotri, A.R. (2010). A model for neural development and treatment of Rett syndrome using human induced pluripotent stem cells. Cell *143*, 527–539.

Mariani, J., Simonini, M.V., Palejev, D., Tomasini, L., Coppola, G., Szekely, A.M., Horvath, T.L., and Vaccarino, F.M. (2012). Modeling human cortical development in vitro using induced pluripotent stem cells. Proc. Natl. Acad. Sci. USA *109*, 12770–12775.

McEvilly, R.J., de Diaz, M.O., Schonemann, M.D., Hooshmand, F., and Rosenfeld, M.G. (2002). Transcriptional regulation of cortical neuron migration by POU domain factors. Science *295*, 1528–1532.

Merkle, F.T., and Eggan, K. (2013). Modeling human disease with pluripotent stem cells: from genome association to function. Cell Stem Cell *12*, 656–668.

Millar, J.K., Pickard, B.S., Mackie, S., James, R., Christie, S., Buchanan, S.R., Malloy, M.P., Chubb, J.E., Huston, E., Baillie, G.S., et al. (2005). DISC1 and PDE4B are interacting genetic factors in schizophrenia that regulate cAMP signaling. Science *310*, 1187–1191.

Miller, J.A., Ding, S.-L., Sunkin, S.M., Smith, K.A., Ng, L., Szafer, A., Ebbert, A., Riley, Z.L., Royall, J.J., Aiona, K., et al. (2014). Transcriptional landscape of the prenatal human brain. Nature *508*, 199–206.

Molyneaux, B.J., Arlotta, P., Menezes, J.R., and Macklis, J.D. (2007). Neuronal subtype specification in the cerebral cortex. Nat. Rev. Neurosci. *8*, 427–437.

Naj, A.C., Jun, G., Beecham, G.W., Wang, L.S., Vardarajan, B.N., Buros, J., Gallins, P.J., Buxbaum, J.D., Jarvik, G.P., Crane, P.K., et al. (2011). Common variants at MS4A4/MS4A6E, CD2AP, CD33 and EPHA1 are associated with late-onset Alzheimer's disease. Nat. Genet. *43*, 436–441.

Neale, B.M., Kou, Y., Liu, L., Ma'ayan, A., Samocha, K.E., Sabo, A., Lin, C.F., Stevens, C., Wang, L.S., Makarov, V., et al. (2012). Patterns and rates of exonic de novo mutations in autism spectrum disorders. Nature *485*, 242–245.

Nicholas, C.R., Chen, J., Tang, Y., Southwell, D.G., Chalmers, N., Vogt, D., Arnold, C.M., Chen, Y.J., Stanley, E.G., Elefanty, A.G., et al. (2013). Functional maturation of hPSC-derived forebrain interneurons requires an extended timeline and mimics human neural development. Cell Stem Cell *12*, 573–586.

Nishida, Y., Adati, N., Ozawa, R., Maeda, A., Sakaki, Y., and Takeda, T. (2008). Identification and classification of genes regulated by phosphatidylinositol 3-kinase- and TRKB-mediated signalling pathways during neuronal differentiation in two subtypes of the human neuroblastoma cell line SH-SY5Y. BMC Res. Notes *1*, 95.

O'Roak, B.J., Vives, L., Girirajan, S., Karakoc, E., Krumm, N., Coe, B.P., Levy, R., Ko, A., Lee, C., Smith, J.D., et al. (2012). Sporadic autism exomes reveal a highly interconnected protein network of de novo mutations. Nature *485*, 246–250.

Obokata, H., Wakayama, T., Sasai, Y., Kojima, K., Vacanti, M.P., Niwa, H., Yamato, M., and Vacanti, C.A. (2014). Stimulus-triggered fate conversion of somatic cells into pluripotency. Nature *505*, 641–647.

Oldham, M.C., Konopka, G., Iwamoto, K., Langfelder, P., Kato, T., Horvath, S., and Geschwind, D.H. (2008). Functional organization of the transcriptome in human brain. Nat. Neurosci. *11*, 1271–1282.

Palmer, T.D., Schwartz, P.H., Taupin, P., Kaspar, B., Stein, S.A., and Gage, F.H. (2001). Cell culture. Progenitor cells from human brain after death. Nature *411*, 42–43.

Paolicelli, R.C., Bolasco, G., Pagani, F., Maggi, L., Scianni, M., Panzanelli, P., Giustetto, M., Ferreira, T.A., Guiducci, E., Dumas, L., et al. (2011). Synaptic pruning by microglia is necessary for normal brain development. Science *333*, 1456–1458.

Parikshak, N.N., Luo, R., Zhang, A., Won, H., Lowe, J.K., Chandran, V., Horvath, S., and Geschwind, D.H. (2013). Integrative functional genomic analyses implicate specific molecular pathways and circuits in autism. Cell *155*, 1008–1021.

Paşca, S.P., Portmann, T., Voineagu, I., Yazawa, M., Shcheglovitov, A., Paşca, A.M., Cord, B., Palmer, T.D., Chikahisa, S., Nishino, S., et al. (2011). Using iPSC-derived neurons to uncover cellular phenotypes associated with Timothy syndrome. Nat. Med. *17*, 1657–1662.

Penzes, P., Cahill, M.E., Jones, K.A., VanLeeuwen, J.E., and Woolfrey, K.M. (2011). Dendritic spine pathology in neuropsychiatric disorders. Nat. Neurosci. *14*, 285–293.

Pinheiro, J., and Bates, D. (2009). Mixed-Effects Models in S and S-PLUS, Second Edition. (New York: Springer).

Plaisier, S.B., Taschereau, R., Wong, J.A., and Graeber, T.G. (2010). Rank-rank hypergeometric overlap: identification of statistically significant overlap between gene-expression signatures. Nucleic Acids Res. *38*, e169.

Rakic, P. (2003). Developmental and evolutionary adaptations of cortical radial glia. Cereb. Cortex *13*, 541–549.

Read, J. (2010). Scalable Multi-label Classification. (Hamilton, New Zealand: University of Waikato).

Ripke, S., O'Dushlaine, C., Chambert, K., Moran, J.L., Kähler, A.K., Akterin, S., Bergen, S.E., Collins, A.L., Crowley, J.J., Fromer, M., et al.; Multicenter Genetic Studies of Schizophrenia Consortium; Psychosis Endophenotypes International Consortium; Wellcome Trust Case Control Consortium 2 (2013). Genome-wide association analysis identifies 13 new risk loci for schizophrenia. Nat. Genet. *45*, 1150–1159.

Ropers, H.H. (2008). Genetics of intellectual disability. Curr. Opin. Genet. Dev. *18*, 241–250.

Rosen, E.Y., Wexler, E.M., Versano, R., Coppola, G., Gao, F., Winden, K.D., Oldham, M.C., Martens, L.H., Zhou, P., Farese, R.V., Jr., and Geschwind, D.H. (2011). Functional genomic analyses identify pathways dysregulated by progranulin deficiency, implicating Wnt signaling. Neuron *71*, 1030–1042.

Ryan, S.D., Dolatabadi, N., Chan, S.F., Zhang, X., Akhtar, M.W., Parker, J., Soldner, F., Sunico, C.R., Nagar, S., Talantova, M., et al. (2013). Isogenic human iPSC Parkinson's model shows nitrosative stress-induced dysfunction in MEF2-PGC1α transcription. Cell *155*, 1351–1364.

Sanders, S.J., Ercan-Sencicek, A.G., Hus, V., Luo, R., Murtha, M.T., Moreno-De-Luca, D., Chu, S.H., Moreau, M.P., Gupta, A.R., Thomson, S.A., et al. (2011). Multiple recurrent de novo CNVs, including duplications of the 7q11.23 Williams syndrome region, are strongly associated with autism. Neuron *70*, 863–885.

Sanders, S.J., Murtha, M.T., Gupta, A.R., Murdoch, J.D., Raubeson, M.J., Willsey, A.J., Ercan-Sencicek, A.G., DiLullo, N.M., Parikshak, N.N., Stein, J.L., et al. (2012). De novo mutations revealed by whole-exome sequencing are strongly associated with autism. Nature *485*, 237–241.

Sandoe, J., and Eggan, K. (2013). Opportunities and challenges of pluripotent stem cell neurodegenerative disease models. Nat. Neurosci. *16*, 780–789.

Soldner, F., Laganière, J., Cheng, A.W., Hockemeyer, D., Gao, Q., Alagappan, R., Khurana, V., Golbe, L.I., Myers, R.H., Lindquist, S., et al. (2011). Generation of isogenic pluripotent stem cells differing exclusively at two early onset Parkinson point mutations. Cell *146*, 318–331.

Sousa, V.H., and Fishell, G. (2010). Sonic hedgehog functions through dynamic changes in temporal competence in the developing forebrain. Curr. Opin. Genet. Dev. *20*, 391–399.

Stolt, C.C., Lommes, P., Sock, E., Chaboissier, M.C., Schedl, A., and Wegner, M. (2003). The Sox9 transcription factor determines glial fate choice in the developing spinal cord. Genes Dev. *17*, 1677–1689.

Strauss, K.A., Puffenberger, E.G., Huentelman, M.J., Gottlieb, S., Dobrin, S.E., Parod, J.M., Stephan, D.A., and Morton, D.H. (2006). Recessive symptomatic focal epilepsy and mutant contactin-associated protein-like 2. N. Engl. J. Med. *354*, 1370–1377.

Takahashi, K., Tanabe, K., Ohnuki, M., Narita, M., Ichisaka, T., Tomoda, K., and Yamanaka, S. (2007). Induction of pluripotent stem cells from adult human fibroblasts by defined factors. Cell *131*, 861–872.

Taylor, S.S., and McKeon, F. (1997). Kinetochore localization of murine Bub1 is required for normal mitotic timing and checkpoint response to spindle damage. Cell *89*, 727–735.

Tsoumakas, G., and Katakis, I. (2007). Multi-Label Classification: An Overview. Int. J. Data Warehous. Min. *3*, 1–13.

Tuoc, T.C., Boretius, S., Sansom, S.N., Pitulescu, M.E., Frahm, J., Livesey, F.J., and Stoykova, A. (2013). Chromatin regulation by BAF170 controls cerebral cortical size and thickness. Dev. Cell *25*, 256–269.

van Bokhoven, H. (2011). Genetic and epigenetic networks in intellectual disabilities. Annu. Rev. Genet. *45*, 81–104.

Vargas, D.L., Nascimbene, C., Krishnan, C., Zimmerman, A.W., and Pardo, C.A. (2005). Neuroglial activation and neuroinflammation in the brain of patients with autism. Ann. Neurol. *57*, 67–81.

Voineagu, I., Wang, X., Johnston, P., Lowe, J.K., Tian, Y., Horvath, S., Mill, J., Cantor, R.M., Blencowe, B.J., and Geschwind, D.H. (2011). Transcriptomic analysis of autistic brain reveals convergent molecular pathology. Nature *474*, 380–384.

Wegiel, J., Schanen, N.C., Cook, E.H., Sigman, M., Brown, W.T., Kuchna, I., Nowicki, K., Wegiel, J., Imaki, H., Ma, S.Y., et al. (2012). Differences between the pattern of developmental abnormalities in autism associated with duplications 15q11.2-q13 and idiopathic autism. J. Neuropathol. Exp. Neurol. *71*, 382–397.

Wexler, E.M., Rosen, E., Lu, D., Osborn, G.E., Martin, E., Raybould, H., and Geschwind, D.H. (2011). Genome-wide analysis of a Wnt1-regulated transcriptional network implicates neurodegenerative pathways. Sci. Signal. *4*, ra65.

Wilkinson, M., Hume, R., Strange, R., and Bell, J.E. (1990). Glial and neuronal differentiation in the human fetal brain 9-23 weeks of gestation. Neuropathol. Appl. Neurobiol. *16*, 193–204.

Willsey, A.J., Sanders, S.J., Li, M., Dong, S., Tebbenkamp, A.T., Muhle, R.A., Reilly, S.K., Lin, L., Fertuzinhos, S., Miller, J.A., et al. (2013). Coexpression networks implicate human midfetal deep cortical projection neurons in the pathogenesis of autism. Cell *155*, 997–1007.

Zambon, A.C., Gaj, S., Ho, I., Hanspers, K., Vranizan, K., Evelo, C.T., Conklin, B.R., Pico, A.R., and Salomonis, N. (2012). GO-Elite: a flexible solution for pathway and ontology over-representation. Bioinformatics *28*, 2209–2210.